Master's thesis

NTNU
Norwegian University of Science and Technology
Faculty of Natural Sciences
Department of Biotechnology and Food Science

Vilde Andrea Tonheim

Exploring the potential of *Corynebacterium glutamicum* to produce the novel compatible solute Di-*myo*-inositol-phosphate

Master's thesis in Chemical Engineering and Biotechnology
Supervisor: Fernando Pérez-García
Co-supervisor: Trygve Brautaset
August 2022

NTNU
Norwegian University of Science and Technology

Vilde Andrea Tonheim

Exploring the potential of *Corynebacterium glutamicum* to produce the novel compatible solute Di-*myo*-inositol-phosphate

Master's thesis in Chemical Engineering and Biotechnology
Supervisor: Fernando Pérez-García
Co-supervisor: Trygve Brautaset
August 2022

Norwegian University of Science and Technology
Faculty of Natural Sciences
Department of Biotechnology and Food Science

Preface

This master thesis was written for the Department of Biotechnology and Food Science at the Norwegian University of Science and Technology. First of all, I would like to thank my supervisor Fernando Pérez-García for always being there to answer my questions, for guiding me through this past year, and for becoming a good friend. I would like to thank Trygve Brautaset for letting me be a part of this research group and my working group for all the support, and for creating a friendly working atmosphere. I would also like to thank Thea Isabel Bakken for being a great friend and lab partner.

Abstract

To combat abiotic stresses, microorganisms accumulate compatible solutes by either *de novo* biosynthesis or uptake from the environment[2]. The intracellular accumulation of these low-molecular weight compounds have been found to increase resistance to osmotic stress, temperature change, oxygen radicals, and radiation, in addition to stabilize the tertiary structure of intracellular macromolecules such as proteins or double-stranded DNA[8][32][11]. Di-*myo*-inositol-phosphate (DIP) is a compatible solute suspected to possess promising features as a UV protectant, moisturizer, PCR enhancer, and DNA protectant[4][5][56][16][45][31]. As of today, compatible solutes are only industrially produced using extremophile microorganisms following inefficient processes. The drawbacks to such processes include shortened lifespan of equipment, reduced volumetric yield, and complicated up and downstream processes[48]. Development of low-salinity fermentation processes is desired, where heterologous expression in mesophile organisms would allow such improvements. The production of DIP has yet to be established in a mesophile system. As the study of extremolytes requires specialized equipment, the establishment of a mesophile system would simplify the production of DIP at the lab-bench scale. *Corynebacterium glutamicum* is a well-established microbial workhorse, best known for its large-scale production of amino acids[49]. It has already been genetically engineered for the production of compatible solutes such as ectoine, hydroxyectoine, mannosylglycerate, and L-pipecolic acid[32][35][49]. In this work, *C. glutamicum* has been genetically engineered for the heterologous expression of the DIP biosynthesis pathway. This was achieved by combining genes from the hyperthermophiles *Thermotoga maritima* and *Pyrococcus furiosus*. To test the newly constructed strains, fermentations in microbioreactors were performed under osmotic and thermal stress. When cultivating the strains in a minimal medium supplemented with 0.5 M or 1.0 M NaCl at 30°C, only the strain carrying the DIP biosynthetic operon from *T. maritima* showed growth improvements with regards to growth rate and biomass formation. Next, a shake flask fermentation, coupled with an osmotic shock down approach was performed for the extraction of compatible solutes including DIP. Finally, the best performing strain was tested in lab-scale bioreactors following the same osmotic shock down approach, proving the feasibility of this bioprocess for the production of non-native compatible

solutes.

Sammendrag

For å motvirke abiotisk stress, akkumulerer mikroorganismer osmobeskyttende molekyler, også kalt osmolytter, ved enten *de novo* biosyntese eller opptak fra omgivelsene[2]. Den intracellulære akkumuleringen av disse molekylene med lav molekylærvekt har vist seg å øke motstanden mot osmotisk stress, temperaturendringer, oksygenradikaler og stråling, i tillegg til å stabilisere tertiærstrukturen til intracellulære makromolekyler som proteiner eller dobbelttrådet DNA[8][32][11]. Di-*myo*-inositol-fosfat (DIP) er en osmolytt som mistenkes å ha lovende egenskaper som UV-beskyttelse, fuktigivning, PCR-forsterkelse og DNA-beskyttelse[4][5][56][16][45][31]. Per i dag produseres osmolytter kun industrielt ved bruk av ekstremofile mikroorganismer via ineffektive prosesser. Ulempene med slike prosesser inkluderer forkortet levetid på utstyr, redusert volumetrisk utbytte og kompliserte opp- og nedstrømsprosesser[48]. Utvikling av fermenteringsprosesser med lav salinitet er ønskelig, der heterolog ekspresjon i mesofile organismer ville tillate slike forbedringer. Produksjonen av DIP er ennå ikke etablert i mesofile mikroorganismer, og ettersom studier av ekstremolytter krever spesialisert utstyr, vil etablering av et mesofilt produksjonssystem forenkle produksjonen av DIP på laboratorie-skala. *Corynebacterium glutamicum* er en veletablert mikrobiell arbeidshest, mest kjent for storskala produksjon av aminosyrer[49]. Bakterien har allerede blitt genetisk modifisert for produksjon av osmolytter som ektoin, hydroksyektoin, mannosylglycerat, og L-pipekolsyre[32][35][49]. I dette arbeidet har en *C. glutamicum* villtype blitt genetisk modifisert for å uttrykke DIP-biosynteseveien. Dette ble oppnådd ved å kombinere gener fra hypertermofilene *Thermotoga maritima* og *Pyrococcus furiosus*. For å teste de nykonstruerte stammene ble fermenteringer i mikrobioreaktorer utført under osmotisk og termisk stress. Ved dyrking av stammene i minimalt medium supplert med 0,5 M NaCl eller 1 M NaCl ved 30°C, er det kun stammen som bærer det DIP-biosyntetiske operonet fra *T. maritima* som viste vekstforbedringer med hensyn til veksthastighet og biomassedannelse. Deretter ble en ristekolbe-fermentering, kombinert med osmotisk-sjokkfall, utført for ekstraksjon av flere osmolytter inkludert DIP. Til sist ble stammen med best ytelse testet i bioreaktorer på laboratorieskala med samme osmotiske sjokkfall tilnærming. Forsøket beviste at den anvendte bioprosessen var funksjonell for produksjon av ikke-native osmolytter.

Contents

1 Introduction

1.1 Compatible Solutes

To survive ever-changing environmental conditions, microorganisms have developed strategies to combat abiotic stresses. To cope with osmotic stress such as high salinity, desiccation, and freezing, a widespread strategy is the ready accumulation of compatible solutes in the cell's cytoplasm. Compatible solutes, also called osmolytes, are low-molecular weight organic molecules, that have low toxicity even at high concentrations[42]. The osmolytes balance the osmotic pressure inside the cells and thus maintain optimum turgor pressure, electrolyte concentration, and cell volume[2]. They can also stabilize the tertiary structure of cellular macromolecules such as proteins, ribosomes, and DNA, without interfering with the metabolism of the cell[32]. This stabilization has been shown to increase the resistance to other types of abiotic stress such as temperature change, oxygen radicals and radiation[8][32][11]. The cell can accumulate compatible solutes by environmental uptake and by *de novo* biosynthesis, and can rapidly regulate the concentration in response to their surroundings[2]. Compatible solutes found in thermophiles and hyperthermophiles are largely different from those found in mesophiles[39]. Commonly, thermophilic and hyperthermophilic extremophiles accumulate negatively charged compatible solutes, as opposed to neutral or zwitterions that are usually found in most microorganisms[42]. Another strategy to cope with osmotic stress is the salt-in strategy[9;53]. It has been found in some extremely halophilic Archaea and Bacteria of the family *Halobacteriaceae* and *Haloanaerobiales*, respectively, in addition to the bacterium *Salinibacter ruber*. The salt-in uses influx of ions from the surroundings, where accumulation of K^+ and Cl^- is dominant[9][53]. The downside to the salt-in strategy is its inflexibility, giving the organism a narrow range of adaptation that disfavors high osmolarity environments[54].

1.2 Common Compatible Solutes

Compatible solutes are either neutral, zwitterionic, or charged, and can be categorized into different substrate classes, such as sugars, amino acids, amino acid derivatives, polyols, or heterosides[23]. They can be found in all three kingdoms of life, where some common compatible solutes are L-proline, ectoine, hydroxyectoine, trehalose, and mannosylglycerate[43]. L-Proline is an amino acid, and thus a zwitterion. The zwitterionic properties form affinity to water, giving proline water-binding abilities (Figure 1.1)[46]. Ectoine is an amino acid derivative, and therefore also a zwitterion. It is an abundance in nature and is often found in halophilic organisms[17]. Ectoine's strong water-binding abilities, and its ability to enhance folding and stabilizes proteins, make the compatible solute interesting for the cosmetic and pharmaceutical industries (Figure 1.2)[16][7]. Some microorganisms also synthesize the ectoine derivative 5-hydroxyectoine (Figure 1.3). In addition to the osmoprotectant abilities shared with ectoine, the derivative has been found to play a role in thermal stress protection[13]. Both L-proline, ectoine, and hydroxyectoine contain nitrogen, and thus can be used as intracellular reserves of carbon, nitrogen, and energy. Under nitrogen-limited growth conditions, such compatible solutes can be metabolized by heterologous organisms, and the synthesis of nitrogenous compatible solutes can be down-regulated in favor of non-nitrogenous compatible solutes[54][12]. One such compound is α-trehalose (Figure 1.4). Trehalose is a non-reducing disaccharide and one of the most widespread compatible solutes found in mesophiles[42][12][21]. The accumulation of anionic carbohydrates is rare in Bacteria, such like α-mannosylglycerate, where the reactive and of the sugar forms glycosidic bonds with a hydroxyl group of glyceric acid (Figure 1.5)[38]. The compatible solute has been found to be favored under thermal stress, and to inhibit thermoprotectant properties[38][49].

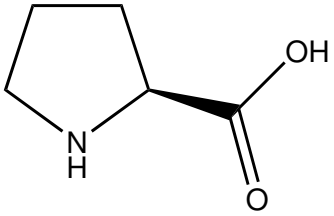

Figure 1.1: The chemical structure of L-proline, in its fully protonated state.

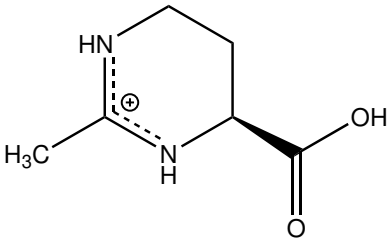

Figure 1.2: The chemical structure of ectoine, in its fully protonated state.

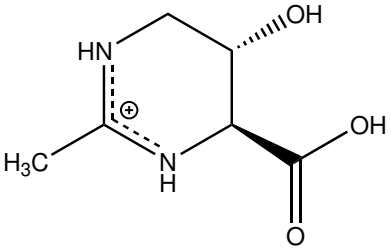

Figure 1.3: The chemical structure of hydroxyectoine, in its fully protonated state.

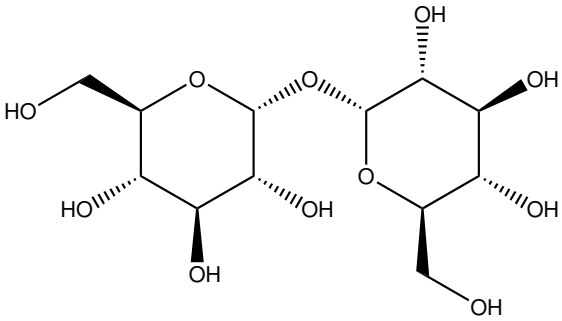

Figure 1.4: The chemical structure of α-trehalose, in its fully protonated state.

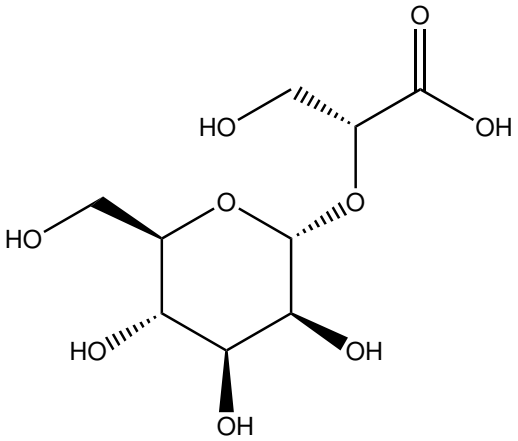

Figure 1.5: The chemical structure of α-mannosylglycerate, in its fully protonated state.

1.3 Industrial Interest and Production

In addition to the osmoprotectant properties, compatible solutes such as ectoine and trehalose have been found to shield against visible light and UVA- and UVB radiation, and to work as skin moisturizers[4][5][56][16]. Additionally, the compatible solutes have been shown to act as PCR enhancers, cell growth promoters in high glucose fermentations, and to preserve biological molecules in pharmaceuticals[45][31]. Such features would be of interest to the cosmetic and pharmaceutical industries.

After experiencing osmotic stress, the compatible solute concentration in the cytoplasm is higher relative to the concentration in optimal conditions. To prevent cell lysis during an osmotic shock-down, most microorganisms have developed mechanosensitive channels that stretch open when the cell membrane experiences supraoptimal turgor pressure[48]. These channels allow rapid efflux of ions and thus can be used for extraction of intracellular compounds, as illustrated in Figure 1.6[26]. This mechanism is utilized in the large-scale commercial production of the compatible solute ectoine. For the production of ectoine in the halophilic bacterium *Halomonas elongata*, the bacterial milking process was established. The process involves high-cell-density fermentation in a high-salinity medium, before separating the cells and resuspending them in MilliQ water to apply an osmotic down-shift. After the release of intracellular compatible solutes, the subsequent reincubation of a high-salinity growth medium recycles the cells for the resynthesizing of ectoine. This alternating high and low osmotic pressure is then repeated to obtain the highest product yield[35][44][52]. Since major cell lysis is prevented, the downstream purification processes are simplified due to the lesser intracellular content in the supernatant. The drawback of the process is the high salt concentration needed for the fermentation of halophilic microorganisms, which promotes corrosion, shortens the lifespan of equipment, reduces volumetric yield, and complicates the downstream processing[48]. Due to the disadvantages of high-salinity fermentation, the development of low-salinity fermentation processes is desirable, and recombinant approaches have been developed[35]. The heterologous expression of compatible solute genes from extremophiles in mesophiles would allow the the production in low to moderate salt concentration fermentations.

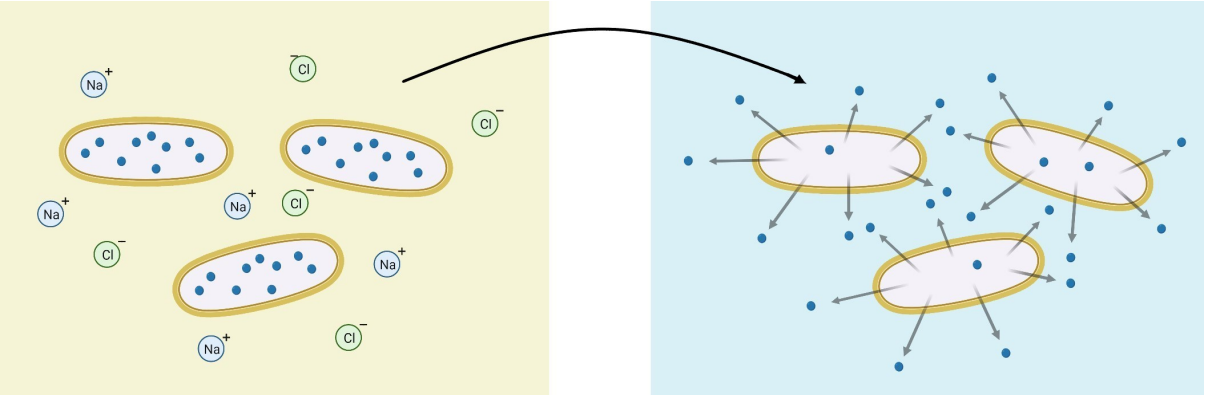

Figure 1.6: Illustration of the osmotic shock down concept. The cells are transferred from a high salinity surroundings to MilliQ water. To balance the downshift of osmotic pressure, the intracellular compounds are secreted from the cells to prevent osmotic lysis. The illustration was created with BioRender.com

1.4 Di-*myo*-Inositol-Phosphate

Di-*myo*-inositol-phosphate (DIP) is a negatively charged compatible solute restricted to hyperthermophiles[14]. It was first discovered in *Pyrococcus woesei* in 1992, and have later been identified in (hyper)thermophilic bacteria in the genera *Thermotoga*, *Rubrobacter* and *Aquifex*, as well as in (hyper)thermophilic archaea, in members of the genera *Methanotorris*, *Thermococcus*, *Pyrodictium*, *Aeropyrum*, *Archaeoglobus*, *Stetteria*, *Hyperthermus*, and *Pyrolobus*[47] [14] [39]. The accumulation of DIP is a typical response to osmotic stress, but have also been shown to increase with supraoptimal temperatures[10]. As of this writing, the limited production of DIP is performed using extremophilic organisms. Due to its shared biological properties as the more studied compatible solutes like ectoine and trehalose, and the fact that DIP is not yet commercialized makes the development of DIP production strategies of interest to cosmetic and pharmaceuticals industries.

The chemical structure of DIP is composed of two molecules of the hexose L-*myo*-inositol, which are connected by a phosphate group. Depending on which carbons are connected, DIP can have three stereochemical configurations; (a) di-*myo*-1,1-inositol-phosphate, (b) di-*myo*-1,3-inositol-phosphate, or (c) di-*myo*-3,3-inositol-phosphate, illustrated in Figure 1.7. Initially, the generally recognized structure was that of (a), but it has later been suggested to recognize isomer (b) instead[41].

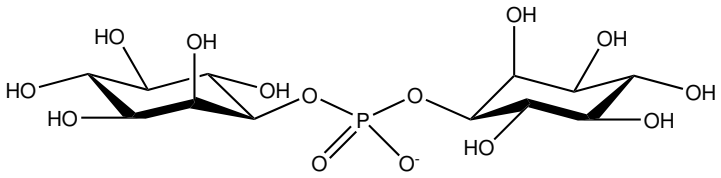

(a) Di-*myo*-1,1-inositol-phosphate

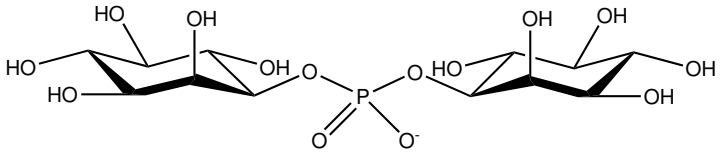

(b) Di-*myo*-1,3-inositol-phosphate

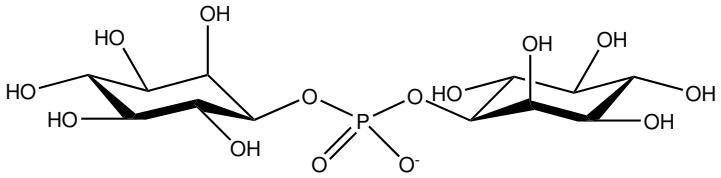

(c) Di-*myo*-3,3-inositol-phosphate

Figure 1.7: The different stereochemical configurations of di-*myo*-inositol-phosphate, where the *myo*-inositol rings is based on the L configuration. The illustration is based on Rodrigues *et al.*,2007[41].

The hyperthermophilic bacteria *Thermotoga maritima*, and the hyperthermophilic archaea *Pyrococcus furiosus*, both synthesises DIP as a native compatible solute in response to supraoptimal temperature and salinity[29][30]. They are both heterotropic and strictly anaerobic and were first discovered in geothermally heated marine sediment of the island Volcano, Italy. *T. maritima* grows at an optimal temperature of 80°C[27], and is slightly halophilic with an optimum NaCl concentration of 2.7 % wt/vol[40]. *P. furiosus* grows at an optimum temperature between 98 to 100 °C, and 3 % wt/vol NaCl, and is strictly dependent on sodium for growth[30]. It has been argued that DIP accumulation in *T. maritima* predominantly responds to an increase in salinity, whereas *P. furiosus* have the same response from increased temperature[30][29]. Generally, purified enzymes of hyperthermophiles have been found to be unstable at the optimal growth temperatures of the organism from which they were extracted[37]. This suggests the need for thermoprotectant compounds, to stabilize cytoplasmic macromolecules and facilitate growth under such extreme conditions. Moreover, the compatible solutes of thermophiles and hyperthermophiles are broadly unique

to the group and have been found to accumulate in higher concentrations when the extremolytes are grown at supraoptimal temperatures[42]. This suggests that they act as thermoprotectants, in addition to their osmoprotectant properties. The drastic accumulation of DIP in *T. maritima*[39] and *P. furiosus*[30][10] in response to increasing temperature is thought to be associated with this thermoprotection[42][39], emphasizing the interest for further investigation around the thermoprotectant abilities of DIP.

1.5 DIP Biosynthesis Pathway

In the DIP biosynthesis pathway four enzymatic activities are required, where D-glucose-6-phosphate is the initial precursor. In the first enzymatic reaction, D-glucose-6-phosphate is converted to L-*myo*-inositol-phosphate catalyzed by *myo*-inositol-1-phosphate-synthease (IPS). In the second reaction, the phosphate is substituted with a cytidine diphosphate by inositol-1-phosphate-cytidylyltransferase (IPCT), yielding CDP-*myo*-inositol. The third reaction is a condensation of L-*myo*-inositol-phosphate and CDP-*myo*-inositol by di-*myo*-inositol-phosphate-phosphate-synthease (DIPPS), forming di-*myo*-inositol-phosphate-phosphate (DIPP). In the fourth and last reaction step, DIPP is dephosphorylated by DIPP-phosphatase (IMP), yielding the final product DIP[14][41]. The DIP synthesis pathway is illustrated in Figure 1.8.

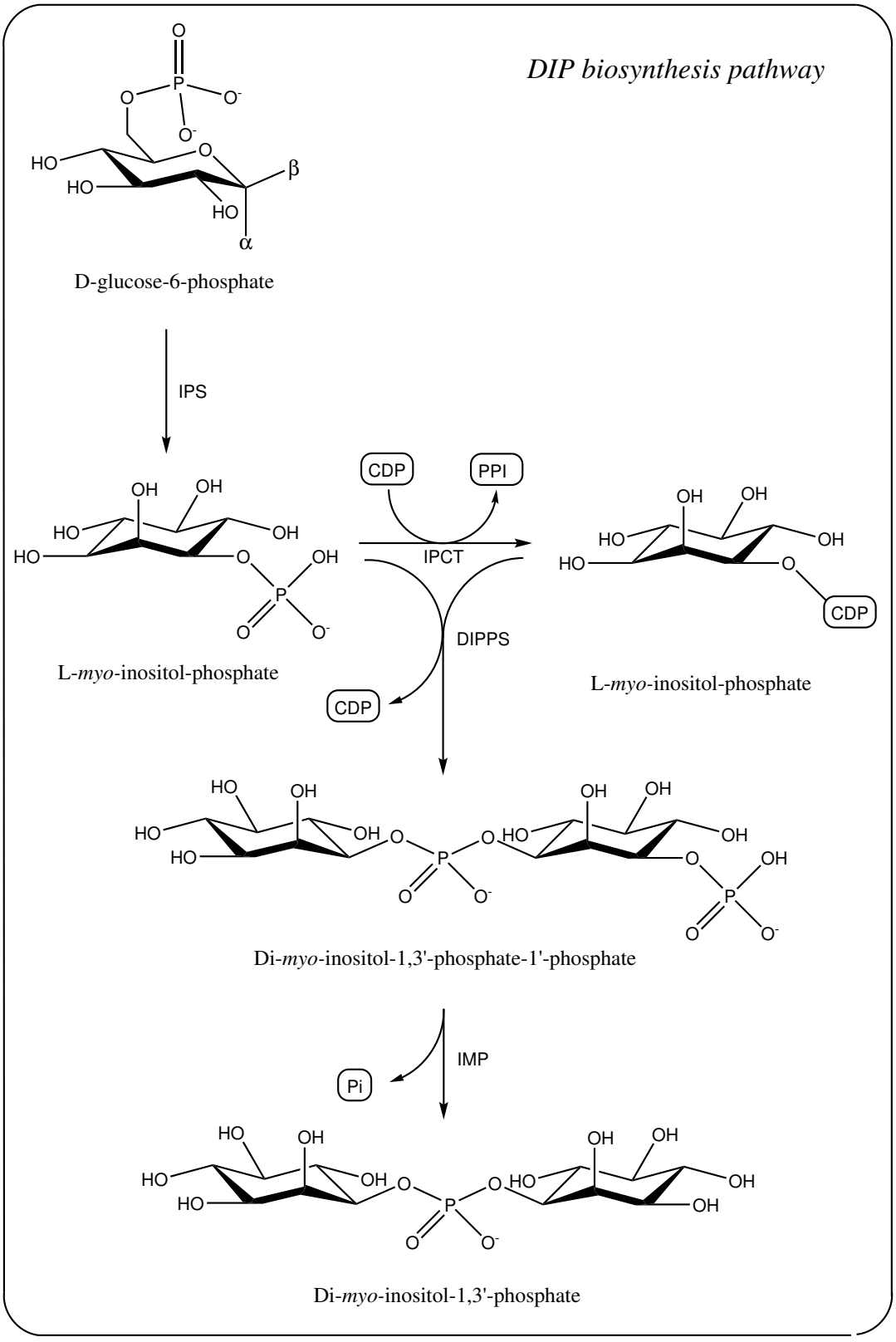

Figure 1.8: Di-*myo*-inositol-phosphate biosynthesis pathway. IPS; *myo*-inositol-1-phosphate-synthease, IPCT; inositol-1-phosphate-cytidylyltransferase, DIPPS; di-*myo*-inositol-phosphate-phosphate-synthease, IMP; di-*myo*-inositol-phosphate-phosphate-phosphatase. The illustration is based on Rodrigues *et al.,* 2007[41].

Homologous genes encoding the IPCT and DIPPS proteins have been found in all organisms accumulating DIP with sequenced genome[41]. Commonly, the genes are fused in a single open reading frame (ORF), which is the case for *P. furiosus*[14]. However, in *T. maritima* the genes are separated and located in the DIP operon together with the *IPS* gene[41][39]. An overview of the DIP synthesis genes are shown in Figure 1.9.

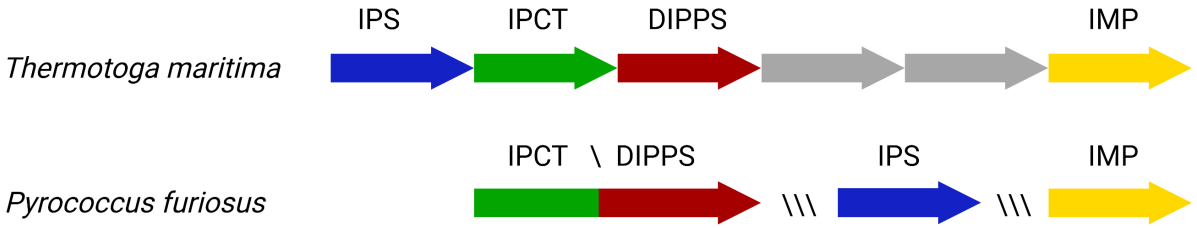

Figure 1.9: Genomic distribution of the DIP biosynthesis pathway genes for *T. maritima* and *P. furiosus*. The ISP, IPCT, and DIPPS genes in *T. maritima* are located in the same operon, where the gene expressing IMP is located in a different genomic region. The IPCT and DIPPS in *P. furiosus* are fused in a bifunctional ORF. The markings \\\ depict discontinuation of genes distribution within *P. furiosus* genome. The illustration is based on Gonçalves *et al.*, 2012[14], and Rodionov *et al.*, 2007[39].

The initial precursor of the DIP biosynthesis pathway is D-glucose-6-phosphate, which is an intermediate in the glycolysis[25]. As a result, the heterologous expression of the DIP biosynthesis pathway redirects the carbon flux away from one of the most widespread central carbon metabolic pathways. The connection between the DIP biosynthesis pathway and the central carbon metabolism is illustrated in Figure 1.10.

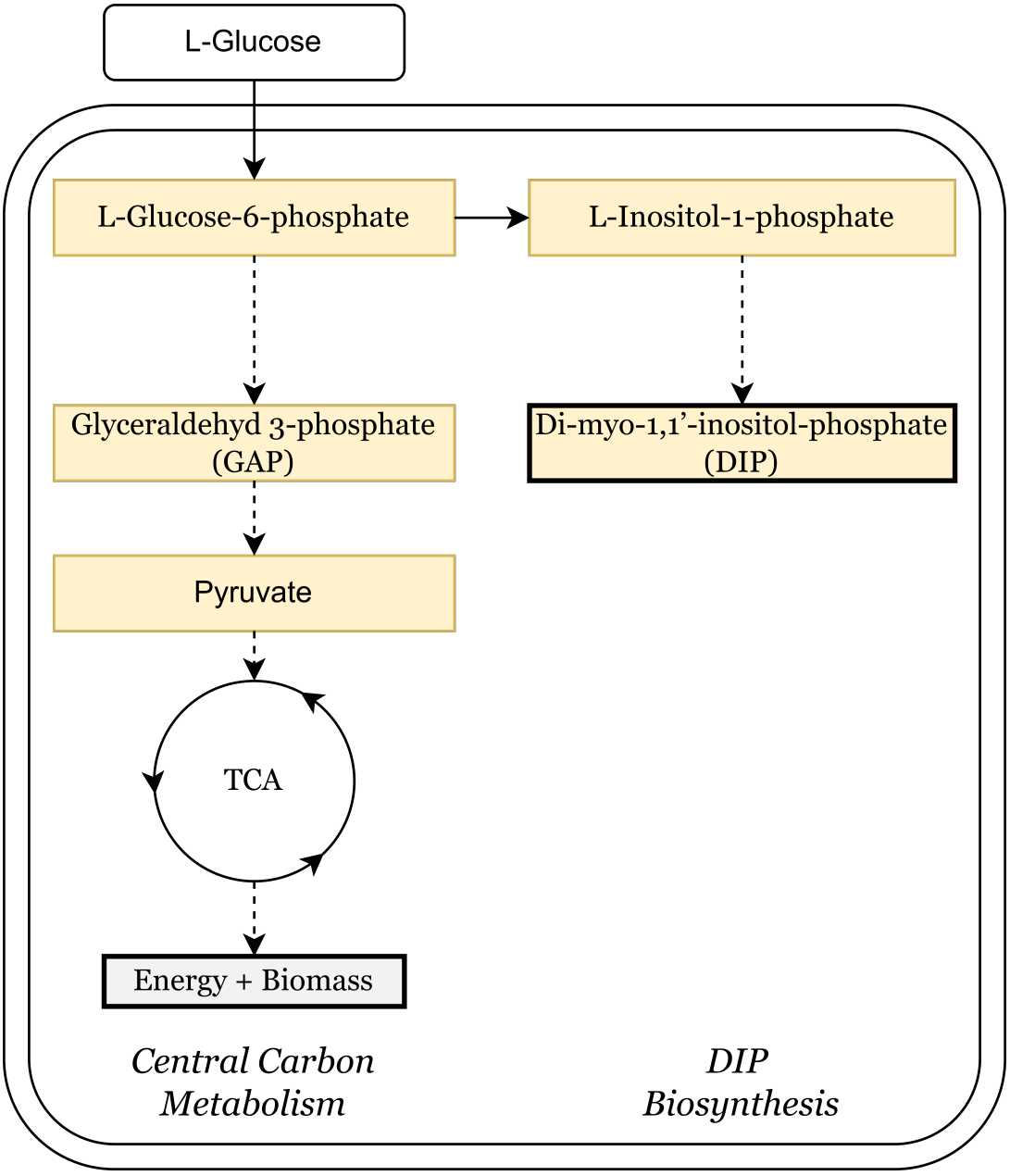

Figure 1.10: Graphical representation of the connection between the central carbon metabolic pathway and the DIP biosynthesis pathway. The illustration is based on Rodionov *et al.*, 2007[39], and is sourced from unpublished work.

1.6 *Corynebacterium Glutamicum*

Corynebacterium glutamicum is a Gram-positive, facultatively anaerobic, and biotin auxotrophic mesophile[28]. It has a coryneform morphology, referring to its distinctive "club-shaped" appearance as shown in Figure 1.11[1]. This soil-bacterium was first discovered at a Japanese zoo in 1956[19], and has later become a well-studied microbial workhorse in biotechnology. It is best known for its large-scale industrial production of amino acids, specially L-glutamate and L-lysine[49]. *C. glutamicum* has also been engineered to produce several modern products, including diamines, alcohols, organic acids, and carotenoids, as well as compatible solutes such as ectoine, L-pipecolic acid, hydroxyectoine and mannosylglycerate[20][35][32][49]. *C. glutamicum* has also been extensively engineered for the consumption of non-native carbon sources including glycerol as a by-product of biodiesel processes, lignocellulosic sugars, and amino sugars from fish industry waste[33]. Moreover, the lack of a complex carbon catabolite repression system enables *C. glutamicum* to consume many substrates in parallel. This differ from other biotechnology workhorses like *Bacillus subtilis* or *Escherichia coli*[15].

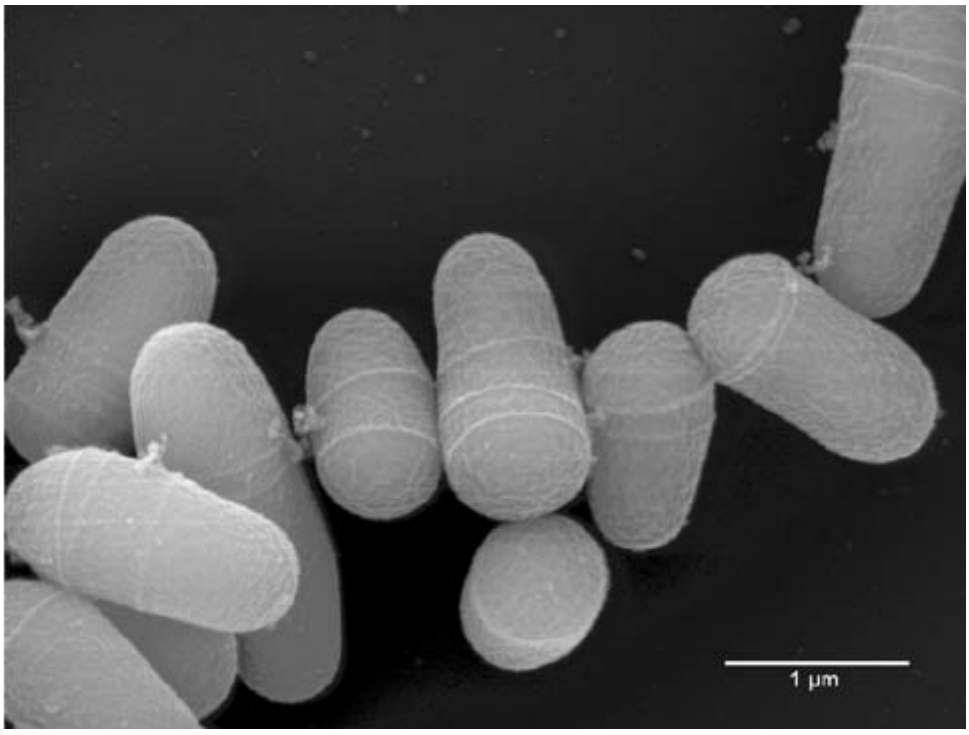

Figure 1.11: Raster electron micrograph of *Corynebacterium glutamicum*. (Krömer, Heinzle and Wittmann 2006, unpublished results)

1.7 Purpose of This Work

This project aims to explore the potential of *C. glutamicum* to produce the compatible solute DIP, by establishing a heterologous expression of the DIP biosynthesis pathway from the hyperthermophiles *T. maritima* and *P. furiosus*. The effect of physiological conditions such as supraoptimal temperatures and salt concentrations will be tested, and the feasibility of scaling-up in bioreactors, coupled with an osmotic shock down approach for extraction, will be explored.

2 Materials and Methods

2.1 Mediums and Solutions

All recipes for the media and solutions used in this work are given in Appendix A.

2.2 Bacterial Strains, Vectors and Growth Conditions

The vectors and stains used in this work are listed in Table 2.1 and Table 2.2, respectively. For the construction of the recombinant vectors, *Escherichia coli* DH5α was used as the cloning host. The vector extractions were done using the ZR Plasmid MinPrep - Classic from Zymo Research, and DNA concentrations were measured using the NanoDrop One from Thermo Scientific. The accuracy of the cloning was proven by DNA sequencing. As the expression and transformation host, *C. glutamicum* ATCC 13032 wild-type was used.

The genes encoding for IPS, IPCT, and DIPPS from *T. maritima* and *P. furiosus*, were assembled in the shuttle vector pVWEX1, yielding the recombinant vectors pVWEX1-DIP-*Tm* and pVWEX1-DIP-*Pf*, respectively. The genes expressing the IMP protein from *T. maritima* and *P. furiosus* were assembled in the shuttle vector pECXT99a, yielding pECXT99a-*imp-Tm* and pECXT99a-*imp-Pf*, respectively. The shuttle vectors used were chosen as they both have isopropyl β-D-1-thiogalactopyranoside (IPTG) inducible promoters. This ensures the simultaneous expression of all genes needed for the DIP biosynthesis pathway. The vectors pVWEx1 and pECXT99a express resistance to the antibiotics kanamycin and tetracycline, respectively, allowing for positive selection.

Throughout this work, *E. coli* was routinely cultivated in LB liquid medium, or on LB agar plates, at 37°C. Pre-cultures of *C. glutamicum* were routinely cultivated in brain heart infusion (BHI) liquid medium, 2TY complex medium, or BHI agar plates at 30°C. The *C. glutamicum* main cultures were done in CGXII minimal medium. The main cultures were inoculated at an initial optical density (OD600) of 1, where 2% glucose was used as the sole carbon source. When necessary, 25 µg/mL kanamycin and 5 µg/mL tetracycline were supplemented to the media. For the induction of the genes cloned, the main cultivation medium was supplemented with 1 mM IPTG. For growth under osmotic stress, a minimal medium was supplemented with either 0.5 M, 1.0 M, or 1.5 M NaCl. All biomass calculations were done using the correlation:
$\mathrm{g/L\ biomass} = 0.343 \cdot \mathrm{OD600}$.

Table 2.1: List of vectors used in this work.

Vector Name	**Description**	**Source**
pVWEx1	Kan^R, *C. glutamicum/E. coli* shuttle vector (P_{taq}, *lacI*, pHM1519 OriVCg)	Peters-Wendisch et al., 2001 [36]
pECXT99a	Tet^R, *C. glutamicum/E. coli* shuttle vector (Ptrc, *lacI*, pGA1, OriVCg)	Kirchner and Tauch 2003 [22]
pVWEx1-DIP-*Tm*	Kan^R, pVWEx1 vector carrying the DIP operon from *Thermotoga maritima*	Tonheim 2021, unpublished*
pECXT99a-*imp-Tm*	Tet^R, pECXT99a vector carrying the *imp* gene from *Thermotoga maritima*	Tonheim 2021, unpublished*
pVWEx1-DIP-*Pf*	Kan^R, pVWEx1 vector carrying the DIP operon from *Pyrococcus furiosus*	This work
pECXT99a-*imp-Pf*	Tet^R, pECXT99a vector carrying the *imp* gene from *Pyrococcus furiosus*	This work

*Unpublished results from TBT4500 - Biotechnology, Specialization Project at NTNU

Table 2.2: List of strains used in this work.

Strain Name	Description	Source
Corynebacterium glutamicum	wild-type strain ATCC 13032, auxotrophic for biotin	Abe 1967[1]
Escherichia coli DH5*α*	Δ*lac*U169 (*ϕ*80*lacZ* ΔM15), *sup*E44, *hsd*R17, *rec*A1, *end*A1, *gyr*A96, *thi*-1, *rel*A1	Hanahan 1983[18]
CgEmpty	*C. glutamicum*(pVWEx1)(pECXT99a)	Tonheim 2021, unpublished*
CgTmTm	*C. glutamicum*(pECXT99a-*imp-Tm*)(pVWEx1-DIP-*Tm*)	Tonheim 2021, unpublished*
CgPfPf	*C. glutamicum*(pECXT99a-*imp-Pf*)(pVWEx1-DIP-*Pf*)	This work
CgTmPf	*C. glutamicum*(pECXT99a-*imp-Tm*)(pVWEx1-DIP-*Pf*)	This work
CgPfTm	*C. glutamicum*(pECXT99a-*imp-Pf*)(pVWEx1-DIP-*Tm*)	This work

*Unpublished results from TBT4500 - Biotechnology, Specialization Project at NTNU

2.2.1 Preservation of Strains

For the preservation of constructed strains, glycerol stocks were made. Overnight precultures of each strain were cultivated in 2TY or BHI complex medium, supplemented with 25 µg/mL kanamycin and 5 µg/mL tetracycline when necessary. The precultures were mixed with 89 % glycerol in a 2:3 ratio, aliquoted in cryo-tubes, and stored at -80 °C. During shorter periods of storage, the strains were kept at -4 °C.

2.3 Molecular Genetic Techniques and Strain Construction

2.3.1 Primers

The primers used for high fidelity polymerase chain reactions (HiFi PCR), and colony PCR, are shown in Table 2.3 and Table 2.4, respectively. The tables show the name, the sequence from 5′ to 3′, and the annealing temperature, for each respective primer, as well as the length of the expected PCR product in base pairs (bps). The primer sequences for the HiFi PCR are marked with different colors and font styles. The black region represents the vector overlapping sequence, the red and italic region represents the ribosomal binding site, the blue and bold region represents

the annealing sequence, and the green and underlined region represents the linker sequence used to join two PCR products in one Gibson assembly. Before use, the primers were resuspended in deionized water to a concentration of 100 µM, and diluted 1:10.

Table 2.3: Name, sequence (5′ → 3′), length of PCR template, and annealing temperature of the primers used in the HiFi PCR. Black; vector overlapping sequence, red and italic; ribosomal binding site, blue and bold; PCR sequence, green and underlined; linker sequence.

Primer Name	Sequence (5′ → 3′)	Length [bps]	Annealing Temperature [C°]
DIPTmFw	GCATGCCTGCAGGTCGACTCTAGAG*GAAAGGAGGCCCTTCAG***ATGGTCAAGGTCCTGATCCTC**	2593	55
DIPTmRw	AATTCGAGCTCGGTACCCGGGGATC**TCACCTGTTGAGCACCAGAAG**		
impTmFw	ATGGAATTCGAGCTCGGTACCCGGG*GAAAGGAGGCCCTTCAG***ATGGACAACGTCGAGAAAAAAACC**	766	53
impTmRw	GCCTGCAGGTCGACTCTAGAGGATC**TCACTTTCCTCCTATTTCTTCTAC**		
ipsPfFw	GCATGCCTGCAGGTCGACTCTAGAG*GAAAGGAGGCCCTTCAG***ATGGTTAGGGTAGCAATTATAG**	1223	51
ipsPfRv	GGGGCGTTCGAA**TCAGAGGTATCTTGGGGGTAGC**		
impct/ dpipsPfFw	**CCAAGATACCTCTGA**TTCGAACGCCCC*GAAAGGAGGCCCTTCAG***ATGAATATCCTTGGAGGTGAGG**	1223	51
impct/ dpipsPfRv	AATTCGAGCTCGGTACCCGGGGATC**TCAACCATTCACATCCCTCC**		
impPfFw	ATGGAATTCGAGCTCGGTACCCGGG*GAAAGGAGGCCCTTCAG***ATGAAGCTTAAGTTCTGGAG**	832	49
impPfRv	GCCTGCAGGTCGACTCTAGAGGATC**CTACTCCAGTAAGCTTAAAATTG**		

Table 2.4: Name, sequence (5′ → 3′), and annealing temperature of the primers used in the colony PCR.

Primer name	Sequence (5′ → 3′)	Annealing temperature [C°]
X1Fw	CATCATAACGGTTCTGGC	49
X1Rv	ATCTTCTCTCATCCGCCA	
ECFw	TTTGCGCCGACATCATAACG	53
ECRv	TACTGCCGCCAGGCAAATTC	

2.3.2 Polymerase Chain Reactions

For the cloning, two protocols of PCR were performed; HiFi PCR, and colony PCR. The HiFi PCR was performed using the CloneAmp™ HiFi PCR premix protocol from Clontech Laboratory. The colony PCR was performed using the GoTaq® PCR protocol from Promega Biotech. The thermal cycling conditions for the CloneAmp PCR and GoTaq® PCR protocols are shown in Table 2.5 and 2.6, respectively. In both protocols, the duration of the extension step depended on the final PCR product expected.

Table 2.5: Thermal cycling conditions for the CloneAmp™ PCR.

Step	**Temperature [°C]**	**Time [sec]**	**Number of Cycles**
Denaturation	98	10	35
Annealing	55	15	35
Extension	72	5 / kb	35
Soak	4	Indefinite	1

Table 2.6: Thermal cycling conditions for the GoTaq® PCR.

Step	**Temperature [°C]**	**Time [min]**	**Number of Cycles**
Initial Denaturation	95	2	1
Denaturation	95	1	35
Annealing	55	1	35
Extension	72	1 / kb	35
Final Extension	72	5	1
Soak	4	Indefinite	1

2.3.3 Gibson Assembly

For the cloning, the Gibson assembly method was used. The vectors were cut using the BamHI HiFi restriction enzyme, with a vector-enzyme ratio of 1 µg : 1 µL. The CutSmart® buffer was used for stabilization. The amount of PCR product and vector depended on their concentration and length. The PCR products should have a concentration of 20 to 30 ng/mL. Deionized water was used to reach the final volume of 5 µL. The mixture was placed in PCR tubes containing 15 µL Gibson master mix, which consists of three different enzymes needed for the assembly. The Gibson assembly was performed with the thermal cycling condition set to 50°C for 1 h.

2.3.4 Transformation of *E. coli* and Colony PRC

To evaluate the Gibson assembly cloning, transformation in *E. coli*, colony PCR, and gel electrophoresis were performed. For the transformation, competent cells of *E. coli* DH5α were defrosted on ice. Then, 10 µL of Gibson reaction was added to the cells, and the mixture was incubated for 15 min on ice. Subsequently, the cells were exposed to a 1.5 min heat shock at 42°C in a thermomixer, followed by a 1 min incubation on ice. Then, 500 µL of LB was added, and the mixture was incubated for 1 hour in a thermomixer, at 37°C and 450 rpm. On selective medium, 100 µL of the mixture was plated, then the remaining suspension was centrifuged for 3 min at 4000 rpm, before the pellets were plated on an additional agar plate. The plates were incubated for 24 hours at 37°C. Following the incubation, colony PCR and gel electrophoresis were performed to screen for positive clones.

2.3.5 Gel Electrophoresis

To evaluate the length of DNA fragments, gel electrophoresis was used. Agarose 0.8% with GelRed was used for the gel, and 1x Tris-acetate-EDTA for the buffer. The standard DNA ladder used to analyze the bands in the gel was Thermo Scientific™ O'GeneRuler 1 kb DNA Ladder, Ready-to-Use- 250-10,000 bp. The gel electrophoresis was run at 100 V and 400 mA, for 30 - 37 min.

2.3.6 *C. glutamicum* Strain Construction

For the preparation of competent cells, overnight pre-cultures of *C. glutamicum* wild-type were inoculated in 5 mL of LB or BHI at 30°C. Following that, 4 x 25 mL BHIS medium were inoculated with 1 mL of the overnight culture and incubated at 30°C for 2-4 hours, until an OD600 of 0.6 was reached. When the specified biomass was achieved, 15 µL of 5 mg/mL ampicillin was added. The cultures were then incubated for 1-1.5 hours at 30°C. Continuing, the cells were constantly kept on ice whenever possible. The suspensions were centrifuged at 4000 rpm for 7 min at 4°C. The supernatant was discarded, and the cells were resuspended with 30 mL of EPB1-buffer, and let sit for 5 min before repeating this centrifugation process three times. Thereafter, the pellets were resuspended in 750 µL EPB2-buffer and aliquoted to 150 mL in microcentrifuge tubes. The competent cells were frozen at -80°C until used.

For the transformation in *C. glutamicum* using low-copy number vectors, 1 mL of BHIS medium was placed in a microcentrifuge tube, and preheated at 46°C. Competent cells of *C. glutamicum* wild-type were put on ice and defrosted, and kept on ice whenever possible during the transformation. The DNA of the modified vector was mixed with the competent cells, where 700 ng of vector was used. The mixtures were incubated for 5-10 min before being transferred to electroporation cuvettes. Electroporation was performed, following the protocol: single pulse, 2.5 Kv, 25 Fv, and 200 Ω. The electroporated cells were mixed with the preheated BHIS and incubated at 46° for 6 min. Subsequently, the mixture was incubated for 1 hour at 30° and 450 rpm in a thermomixer. The mixture was then centrifuged for 3 minutes at 5000 rpm, and the pellets were plated on selective BHI agar plates. The plates were incubated for 1-2 days at 30°C.

2.4 Growth Experiments

During the growth experiments, three parallels of each strain were used to calculate the averages ($\bar{x}$) and the standard deviations (S_x). For the calculations of S_x, the Equation B.2 was used. The average $\bar{x}$ was calculated using Equation B.3, and the biomass yield was calculated using Equation B.4. The calculations are shown in Appendix B.3. The recombinant strains were grown under osmotic and thermal stress to evaluate the effect of the heterologous DIP biosynthesis. The raw growth data is found in Appendix C.

2.4.1 Preparation and Inoculation

For the preparation of overnight pre-cultures for the growth experiments, shake flasks containing 25 mL of 2TY medium were inoculated. The media were supplemented with 25 µg/mL kanamycin and 5 µg/mL tetracycline when needed. The pre-cultures were incubated at 30°C. The OD600 of the cultures was measured, from which the volumes needed to achieve an OD600 of 1 in the main medium were calculated. The Equation B.1 was used, and is shown in Appendix B. The calculated volumes of preculture were transferred to falcon tubes and centrifuged for 7 min at 4000 rpm. The supernatants were discarded, the cells resuspended and washed with CGXII salt solution, and the suspensions were centrifuged for 7 min, at 4000 rpm. The supernatants were again discarded, and the cells were resuspended in CGXII minimal medium before inoculating the main cultivation medium.

2.4.2 Microbioreactor

To evaluate the growth of the constructed strains under thermal and osmotic stress, six fermentations were performed using a microbioreactor (BioLector Pro® from m2p-labs pat of Beckman Coulter Life Sciences). They were performed in the 1 mL 48-well microtiter FlowerPlate for online cultivation, with clear bottoms for automatic biomass measurements. An adhesive gas-permeable sealing foil was used to prevent contamination and to permit aerobic conditions. The stirring rate of 1100 RPM was used as a set-point. Three osmotic stress experiments were performed at 30 °C, where the growth in minimal medium supplemented 0.5 M, 1.0 M, and 1.5 M NaCl were

tested. Three thermal stress experiments were performed with no added osmotic stress, and under different temperatures of respectively 30°C, 40°C, and 50°C. After the carbon source was depleted, and the growth reached the stationary phase, samples used for OD600 measurement and HPLC analysis, were taken from the parallels that grew. The average of the last 30 automatic biomass measurements taken by the BioLector, and the OD600 measurement of the finished fermentation, were used to calculate the OD600 correlation factor (CF_{OD}). By multiplying the CF_{OD} with the biomass data from the BioLector, real biomass values were obtained. The (CF_{OD}) for each fermentation were calculated using the Equation B.5 as described in Appendix B.4, and are listed in Table C.5.

2.4.3 Shake Flasks

For the shake flask growth experiment, 50 mL CGXII minimal media supplemented with 0.5 M NaCl was inoculated and incubated at 30 °C for 20 hours. Subsequently, an osmotic shock down was used for the extraction of compatible solutes. Samples used for OD600 measurement and HPLC analysis were taken continuously throughout the fermentation, and incubation during the osmotic shock down. The osmotic shock down concept is illustrated in Figure 1.6.

2.4.4 Bench-top Bioreactor

For the up-scaling of the fermentations, bench-top bioreactors (Microbial Bioreactor 1 L Dished-Bottom from Applikon Biotechnology) were used. The autoclavable baffled glass reactor had a 1.25 L total volume, 0.9 L working volume, and two four-bladed Rushton impellers with an outer diameter of 45 mm. The pO2- and pH levels were monitored using 12 mm polarographic DO2 sensors (AppliSens) and 12 mm pH sensors (AppliSens), respectively. A pO2 set-point of 30 % of maximum dissolved oxygen was used, which was maintained automatically by the change of stirring rate. A pH of 7 was used as a set-point and was maintained automatically by the addition of either 10 % w/w phosphoric acid, or 5 M potassium hydroxide. An aeration rate of 0.75 vvm of air was used, and bobbled through the medium using a L-type sparger. The temperature was kept at 30°C by an inner cooling system and an outer heating jacked in contact with the glass bioreactor vessel. Overnight shake flask pre-cultures

in 2TY complex medium were used to inoculate a working volume of 500 mL minimal medium supplemented with 0.5 M NaCl, to an OD600 of 1. The minimal medium did not contain the buffer MOPPS as the bioreactor used an automatic pH control system. Samples used for OD600 measurement and HPLC analysis, were aseptically collected using the Super Safe Sampler device from the company Infors HT.

2.4.5 Osmotic Shock Down

For the extraction of intracellular compatible solutes, an osmotic shock down was performed on both the osmotic stress growth experiments in shake flask and bioreactor. The cells are grown under osmotic stress for the accumulation of compatible solutes such as DIP. The entirety of the cultures was centrifuged at 4000 rpm for 10 minutes, before 1 mL samples of the supernatants were taken. The pellets were then washed with CGXII salt solution, and resuspended in MilliQ water until the volume equaled the volume of the culture from which the pellets were separated from, before the suspensions were incubated at 30°C. Samples of 1 mL from the osmotic shock down suspension in the shack flasks fermentation and the bioreactor fermentation, were taken every second hour and hourly, respectively. The samples were used for OD600 measurement and HPLC analysis. The suspensions from the shake flask experiment and the bioreactor experiment, were incubated 30°C for 72 h (3 days) and 24 h, respectively. The osmotic shock down concept is illustrated in Figure 1.6.

2.4.6 OD600 Measurements

The OD600 of the cultures was measured using a spectrophotometer (WPA CO 8000 Biowave Cell Density Meter from Biochrom Ltd). The samples were measured every second hour or hourly. The OD600 measurements were used to calculate the final biomass and growth rate, where the raw data and the calculations are shown in Appendix C and B, respectively.

2.5 High-Performance Liquid Chromatography

For the quantification of extracellular carbohydrates, a high-performance liquid chromatography (HPLC) system was used (Waters Alliance e2695 Separations Module). Supernatants from the cultures used in the successful osmotic stress growth experiments, were sampled before and after performing an osmotic shock down. The samples were diluted 1:10 before being analyzed and stored at -20°C. The quantification of carbohydrates was performed using a 300 × 7.8 mm Hi-plex (Agilent, Germany) pre-warmed to 45°C, and detected by a refractive index detector (2414 RI Detector, Waters). For the mobile phase, 5 mM sulfuric acid was used at a flow rate of 0.6 mL/min.

3 Results

3.1 Strains Performance Evaluation in Microbioreactor

To study the growth of the newly constructed strains, and the effect of thermal and osmotic stress, fermentations in microbioreactors were performed. The strains CgEmpty, CgTmTm, CgPfPf, CgTmPf, and CgPfTm were grown in regular minimal medium at 30°C, 40°C, and 50°C, as well as in minimal medium supplemented with 0.5 M, 1.0 M, and 1.5 M NaCl at 30°C. OD600 measurements were taken after the fermentations ended, and used to correlate the automatic biomass measurements taken by the BioLector to real values. The correlation factors (CF_{OD}) for each fermentation were calculated using the Equation B.5 as described in Appendix B.4, and are listed in Table C.5.

To be able to compare the microbioreactor growth data to the shake flask and bench-top bioreactor growth data, a microbioreactor correlation factor (CF_{Micro}) must be calculated and multiplied by the growth rates from the BioLector fermentations. The CF_{Micro} is found by dividing the average growth rate of CgEmpty in shake flasks ($\overline{GR}_{\text{Shake flasks}}$) in optimal conditions, by the average growth rate of CgEmpty in microbioreactors ($\overline{GR}_{\text{Micro}}$) at the same conditions. This was done using the Equation B.6 as described in Appendix B.5. The average growth rates used are listed in Table C.1.

3.1.1 Testing Growth Performance of the Newly Constructed Strains Under Different Cultivation Temperatures

All strains grew at the optimum temperature of 30°C, as shown in Figure 3.1. The control strain carrying the empty vectors (also named CgEmpty), had the shortest lag phase, the highest growth rate of 0.40 ± 0.01 h^{-1}, final biomass of 10.06 ± 0.40 g/L and biomass yield of 0.50 ± 0.02 g/g. The modified strains CgTmTm and CgPfTm (Table 2.2) followed a similar growth behavior to each other, as did the strains CgPfPf and CgTmPf (Table 2.2). The strains CgTmTm and CgPfTm had a slightly longer lag phase than the control strain, and a similar growth rates of 0.37 ± 0.01 h^{-1} and 0.37 ± 0.02 h^{-1}, final biomasses of 9.38 ± 0.40 g/L and 9.60 ± 1.19 g/L, and biomass yields of 0.47 ± 0.02 g/g and 0.48 ± 0.00 g/g, respectively. The strains CgPfPf and CgTmPf had a significantly longer lag phase than the other strains, and the lowest growth rates of 0.29 ± 0.02 h^{-1} and 0.29 ± 0.02 h^{-1}, final biomasses of 9.60 ± 0.00 g/L and 9.83 ± 0.40 g/L, and biomass yields of 0.49 ± 0.02 g/g and 0.48 ± 0.06 g/g, respectively. Due to the overlapping uncertainties, the final biomasses and biomass yields of the strains overexpressing the DIP biosynthesis pathway have no significant differences. The total change in biomass and the growth rate values for all strains which grew at 30° are shown in Figure 3.3, and their values are listed in Table 3.1.

During the fermentation with the supraoptimal temperature of 40°C, only the control strain CgEmpty grew with a growth rate of 0.10 ± 0.02 h^{-1}, final biomass of 0.86 ± 0.17 g/L, and a biomass yield of 0.04 ± 0.01 g/g. The growth curve is shown in Figure 3.2, and the growth rate, final biomass, and biomass yield are listed in Table 3.1. The total change in biomass and the growth rate are shown compared to each other in Figure 3.3. As none of the strains tested were able to grow at 50°C, no results are presented from this fermentation.

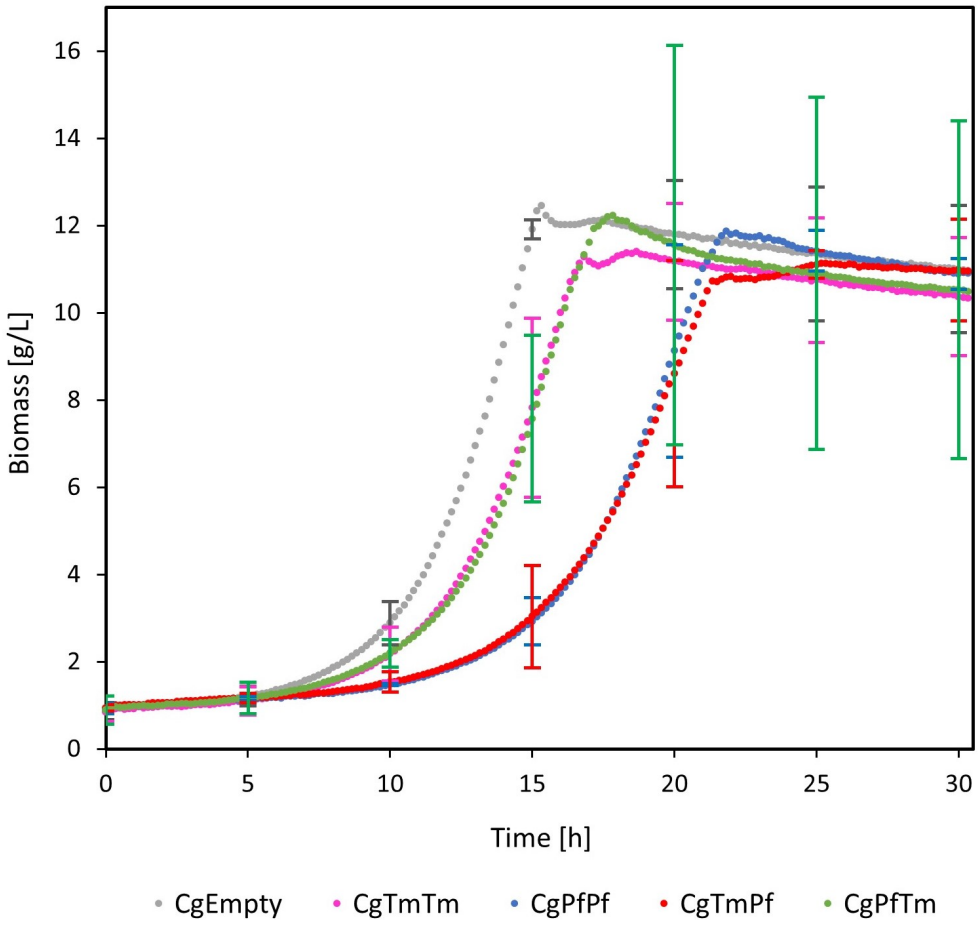

Figure 3.1: Growth curves from the BioLector fermentation in regular minimal medium at 30°C, where the average biomass of the different strains are plotted against the fermentation time. When possible, average and standard deviation values are shown.

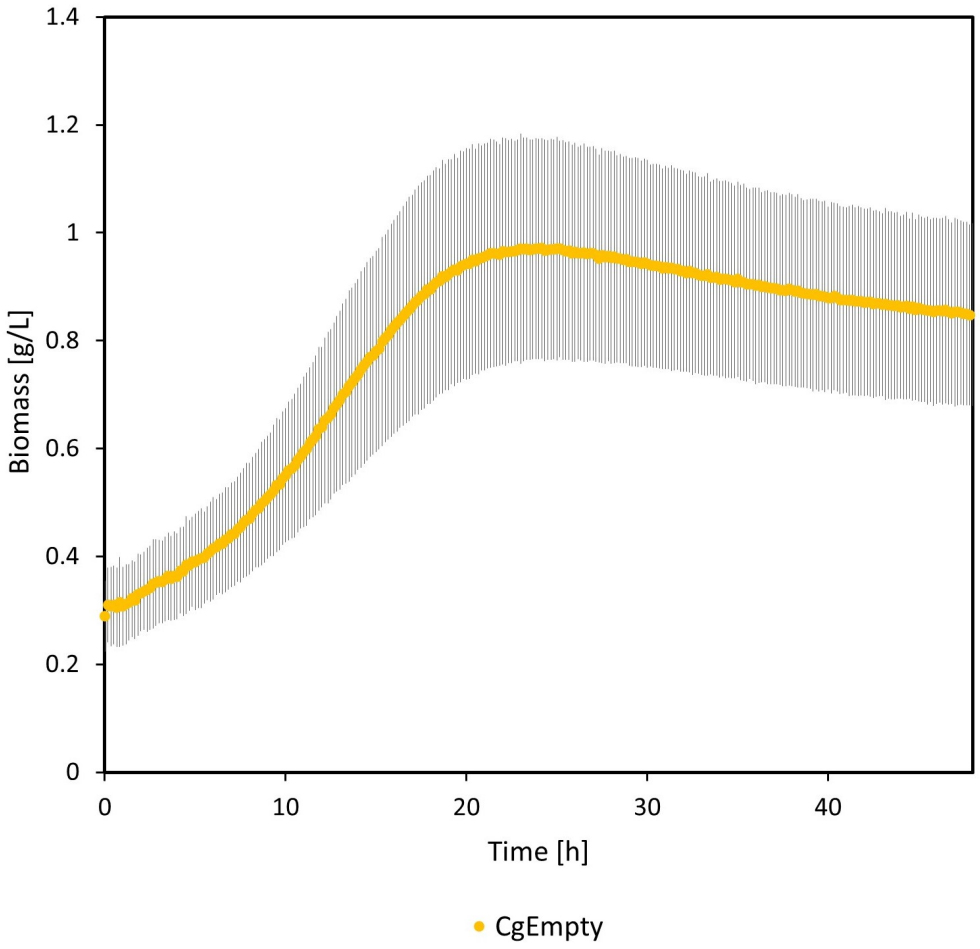

Figure 3.2: Growth curve from the BioLector fermentation grown in regular minimal medium at 40°C, where the average biomass of CgEmpty is plotted against the fermentation time. Average and standard deviation values are shown.

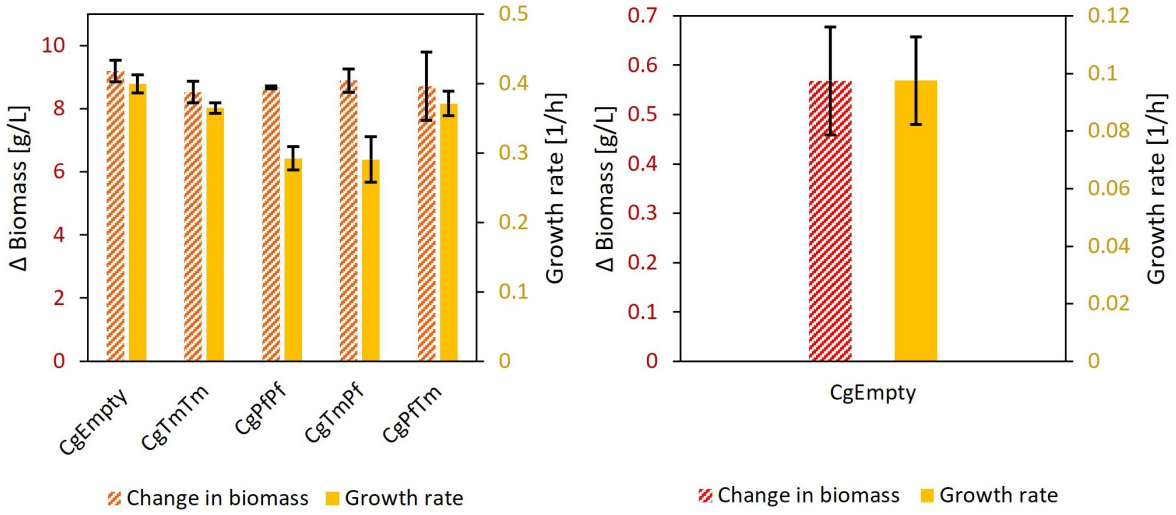

Figure 3.3: Results from the BioLector fermentation at 30°C (Left), and at 40°C (Right). The striped columns show the average total change in biomass, and the solid colored columns show the average growth rate of the strains. Average and standard deviation values are shown.

Table 3.1: Results from the BioLector fermentations in regular minimal medium at 30°C and 40°C. The values show the average growth rate, the average final biomass and the average biomass yield of the strain parallels. The average and standard deviation values are listed. The biomass yield was calculated based on 20 g/L glucose used as sole carbon source.

Strain Name	**Growth Rate [h^{-1}]**	**Final Biomass [g/L]**	**Biomass Yield [g/g]**
Temperature of 30 °C			
CgEmpty	0.40 ± 0.01	10.06 ± 0.40	0.50 ± 0.02
CgTmTm	0.37 ± 0.01	9.38 ± 0.40	0.47 ± 0.02
CgPfPf	0.29 ± 0.02	9.60 ± 0.00	0.48 ± 0.00
CgTmPf	0.29 ± 0.03	9.83 ± 0.40	0.49 ± 0.02
CgPfTm	0.37 ± 0.02	9.60 ± 1.19	0.48 ± 0.06
Strain Name	**Growth Rate [h^{-1}]**	**Final Biomass [g/L]**	**Biomass Yield [g/g]**
Temperature of 40 °C			
CgEmpty	0.10 ± 0.02	0.86 ± 0.17	0.04 ± 0.01
CgTmTm	-	-	-
CgPfPf	-	-	-
CgTmPf	-	-	-
CgPfTm	-	-	-

3.1.2 Testing Growth Performance of the Newly Constructed Strains Under Different Osmotic Pressure Conditions

All strains tested grew in minimal medium supplemented with 0.5 M NaCl, as seen in Figure 3.4. The control strain CgEmpty grown in regular minimal medium reached the highest growth rate, final biomass, and biomass yield of 0.44 ± 0.01 h^{-1}, 9.83 ± 0.40 g/L, and 0.49 ± 0.02 g/g, respectively. The control strain cultivated in minimal medium supplemented with 0.5 M NaCl reached a growth rate of 0.13 ± 0.01 h^{-1}, final biomass of 8.00 ± 0.40 g/L, and biomass yield of 0.40 ± 0.02 g/g. The strains CgPfPf and CgTmPf shared identical growth rates of 0.13 ± 0.00 h^{-1}, had final biomasses of 9.38 ± 0.40 g/L and 8.67 ± 0.02 g/L, and biomass yields of 0.47 ± 0.02 g/g and 0.48 ± 0.00 g/g, respectively. The strains CgTmTm and CgPfTm were the only engineered strains to show a higher growth rate than the control strain grown with 0.5 M NaCl supplemented, with the respective growth rates of 0.15 ± 0.00 h^{-1} and 0.14 ± 0.01 h^{-1}. Their final biomasses and biomass yields were 8.23 ± 0.00 g/L and 8.92 ± 0.69 g/L, and 0.41 ± 0.00 g/g and 0.45 ± 0.03 g/g, respectively. After entering the stationary phase, all strains showed a decreasing growth behavior. The final biomass should preferably be calculated after the strains show a more stable behavior often associated with the stationary phase. The final biomass and biomass yield values can therefore be unrepresentative of the growth, and should be seen in comparison to the growth curve shown in Figure 3.4. All values from the growth experiment are listed in Table 3.2. The total change in biomass, and the growth rate for all strains which grew in this fermentation, are shown in Figure 3.6.

During the fermentation in minimal medium supplemented with 1.0 M NaCl, only the control strain, and one parallel from each of the strains CgTmTm, CgTmPf and CgPfTm grew. The strain CgPfTm had a small growth rate of 0.02 h^{-1}, a final biomass of 0.34 g/L, and a biomass yield of 0.02 g/g. The strains CgTmTm and CgTmPf had both a growth rate of 0.03 h^{-1}, final biomasses of 2.40 g/L, and 2.06 g/L, and biomass yields of 0.12 g/g and 0.10 g/g, respectively. The growth is shown in Figure 3.5. Looking at the growth curve of CgTmTm, the fermentation is ended before a clear stationary phase is reached, thus the biomass of CgTmTm listed in Table 3.2 is not representative of the final biomass. The control strain grown without NaCl added to

the medium, had a growth rate of 0.21 $\pm$ 0.01 h^{-1}, a final biomass of 5.37 $\pm$ 0.20 g/L, and a biomass yield of 0.27 $\pm$ 0.01 g/g. Compared to the two previous microbioreactor fermentations of the control strain with no NaCl added at 30°C, the significantly lower growth rate and final biomass indicate that the experiment was compromised due to unidentified technical errors. The total change in biomass, and the growth rate values for all strains which grew with 1.0 M NaCl supplemented, are shown in Figure 3.6, and their values are listed in Table 3.2. As neither of the strains overexpressing the DIP biosynthesis pathway was able to grow with 1.5 M NaCl supplemented, no results are shown from this fermentation.

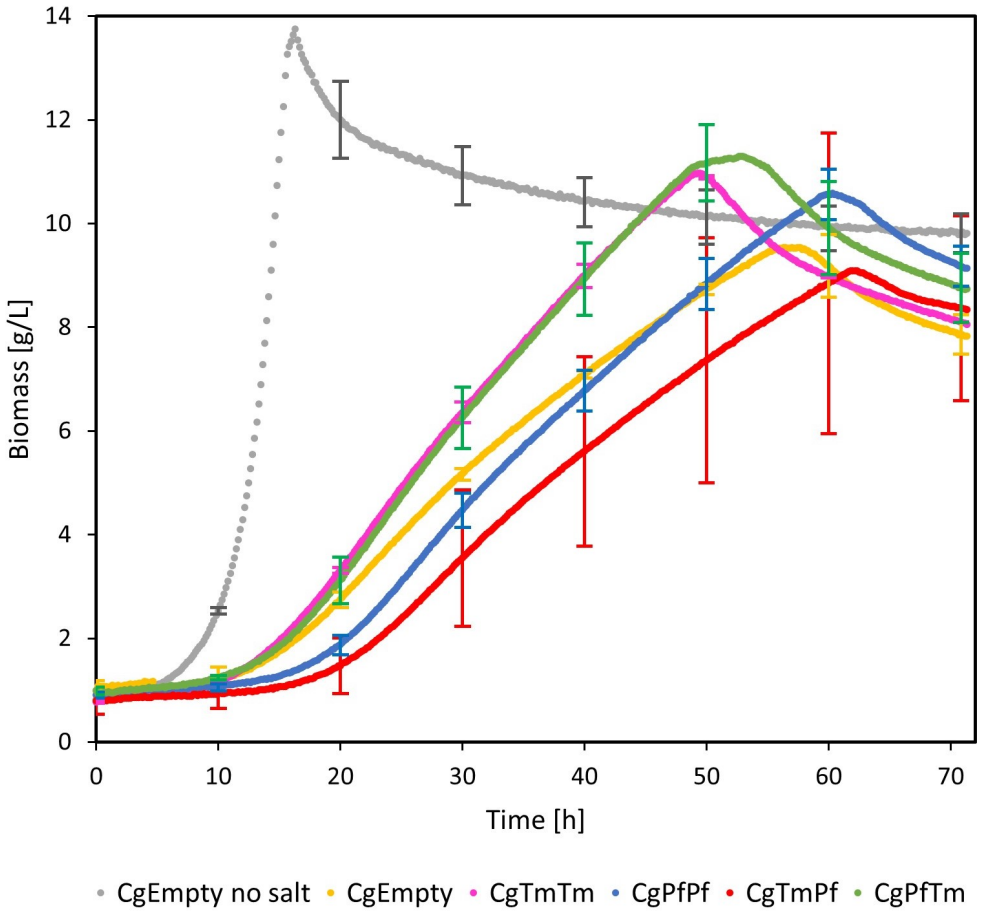

Figure 3.4: Growth curves from the BioLector fermentation grown in minimal medium supplemented with 0.5 M NaCl at 30°C, where the average biomasses of the different strains are plotted against the fermentation time. Growth curve of CgEmpty at 30°C in regular minimal medium is also depicted (grey dots). When possible, average and standard deviation values are shown.

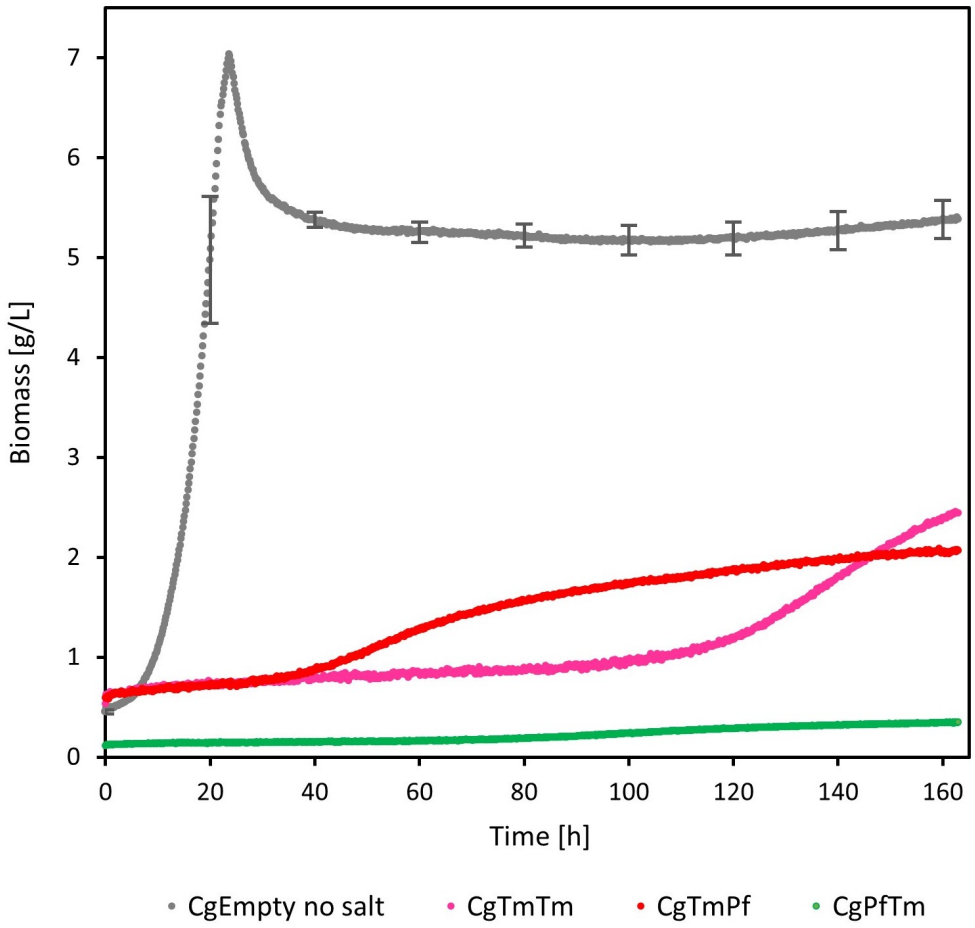

Figure 3.5: Growth curves from the BioLector fermentation in minimal medium supplemented with 1.0 M NaCl at 30 °C, where the biomasses of the different strains are plotted against the fermentation time. Growth curve of CgEmpty at 30°C in regular minimal medium is also depicted (grey dots). When possible, average and standard values are shown.

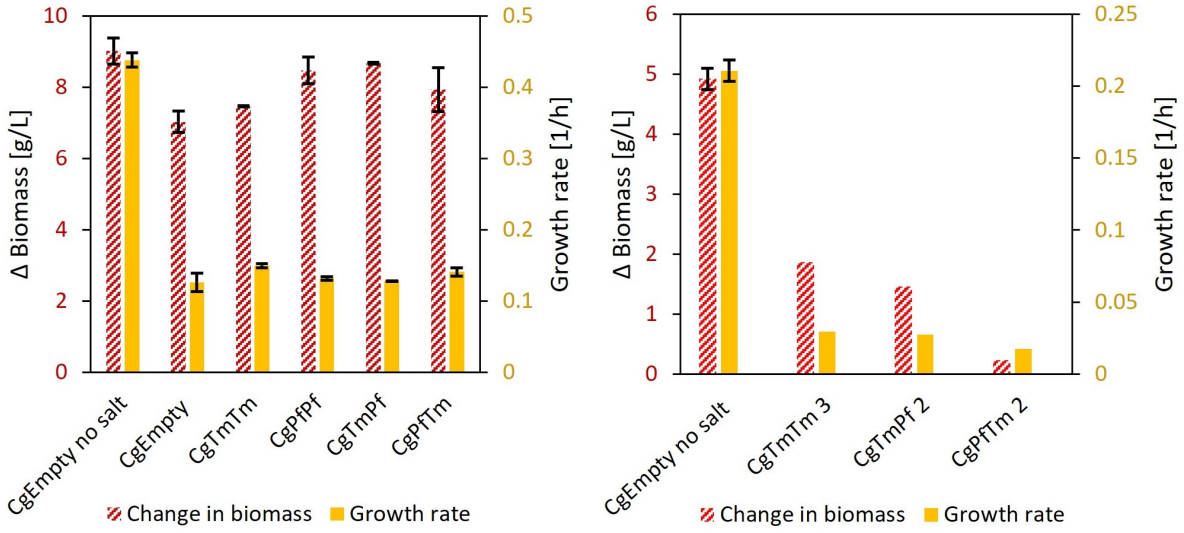

Figure 3.6: Results from the BioLector fermentation grown in minimal medium supplemented with 0.5 M NaCl (Left), and with 1.0 M NaCl (Right), at 30°C. The striped columns show the average total change in biomass, and the solid colored columns show the average growth rate. When possible, average and standard deviation values are shown.

Table 3.2: Results from the BioLector fermentations in minimal medium supplemented with 0.5 M NaCl and 1.0 M NaCl, at 30 °C. The values show the average growth rate, average final biomass and average biomass yield of the strain parallels. The average and standard deviation values are listed. The biomass yields were calculated based on 20 g/L glucose as sole carbon source.

Strain Name	**Growth rate [h^{-1}]**	**Final biomass [g/L]**	**Biomass yield [g/g]**
NaCl concentration of 0.5 M			
CgEmpty no salt	0.44 ± 0.01	9.83 ± 0.40	0.49 ± 0.02
CgEmpty	0.13 ± 0.01	8.00 ± 0.40	0.40 ± 0.02
CgTmTm	0.15 ± 0.00	8.23 ± 0.00	0.41 ± 0.00
CgPfPf	0.13 ± 0.00	9.38 ± 0.40	0.47 ± 0.02
CgTmPf ⋆	0.13 ± 0.00	8.67 ± 0.02	0.48 ± 0.00
CgPfTm	0.14 ± 0.01	8.92 ± 0.69	0.45 ± 0.03
Strain Name	**Growth rate [h^{-1}]**	**Final biomass [g/L]**	**Biomass yield [g/g]**
NaCl concentration of 1.0 M			
CgEmpty no salt	0.21 ± 0.01	5.37 ± 0.20	0.27 ± 0.01
CgEmpty	-	-	-
CgTmTm †	0.03	2.40	0.12
CgPfPf	-	-	-
CgTmPf †	0.03	2.06	0.10
CgPfTm †	0.02	0.34	0.02

⋆ Results from only two parallels.† Results from only one parallel.

3.2 Application of Osmotic Shock Down Approach for The Production of Compatible Solutes

For the production of compatible solutes, the process of bacterial milking or osmotic shock down was adapted and used in this thesis[44] [34]. Since the constructed strains grew best at 30°C, and with 0.5 M NaCl in the microbioreactors, these conditions were used during the scale-up into a shake flask growth experiment with 50 mL of working volume. The strains CgTmTm and CgPfTm (Table 2.2) showed the most promising behavior, and thus were used in this experiment in addition to the control strain CgEmpty (Table 2.2). After growing the cells in minimal medium with 2% glucose as the sole carbon source supplemented with 0.5 M NaCl at 30°C, the cells were collected via centrifugation and washed with CGXII salt solution, before being resuspended in MilliQ water until the volume equaled the volume of the culture from which the pellets were separated from. An illustration of the osmotic shock down concept is shown in Figure 3.7. During the fermentation in minimal medium supplemented with 0.5 M NaCl, the cells should accumulate intracellular compounds, which should theoretically be secreted when transferred to water. The growth curves of the strains are shown in Figure 3.8. The control strain CgEmpty had a growth rate of 0.17 ± 0.01 h^{-1}, and a biomass of 2.97 ± 0.71 g/L. The strain CgTmTm had an equal growth rate of 0.17 ± 0.00 h^{-1}, and a biomass of 2.63 ± 0.20 g/L. The strain CgPfTm had the lowest growth rate of 0.15 ± 0.00 h^{-1}, and biomass of 2.63 ± 1.03 g/L. It is been previously found that α-mannosylglycerate in *Rhodothermus* spp. increase during the exponential phase, and abruptly decrease when the cells enter the stationary phase[50]. Both DIP and α-mannosylglycerate are negatively charged compatible solutes. In addition, DIP is a growth-related molecule, and it is as of this writing not known if DIP can be degraded or consumed. As a high intracellular concentration of DIP is desired, the fermentation was ended in what was believed to be the end of the logarithmic phase based on a previously unpublished growth experiment. Due to the early transfer to water in conjunction with the osmotic shock down, the final biomass and growth curve do not represent the potential of the strains as the carbon source was not depleted. The biomass yields are therefore not calculated. The growth values are listed in Table 3.3. The OD600 measurements used to make the growth curve are listed in Table C.2, found in Appendix C.

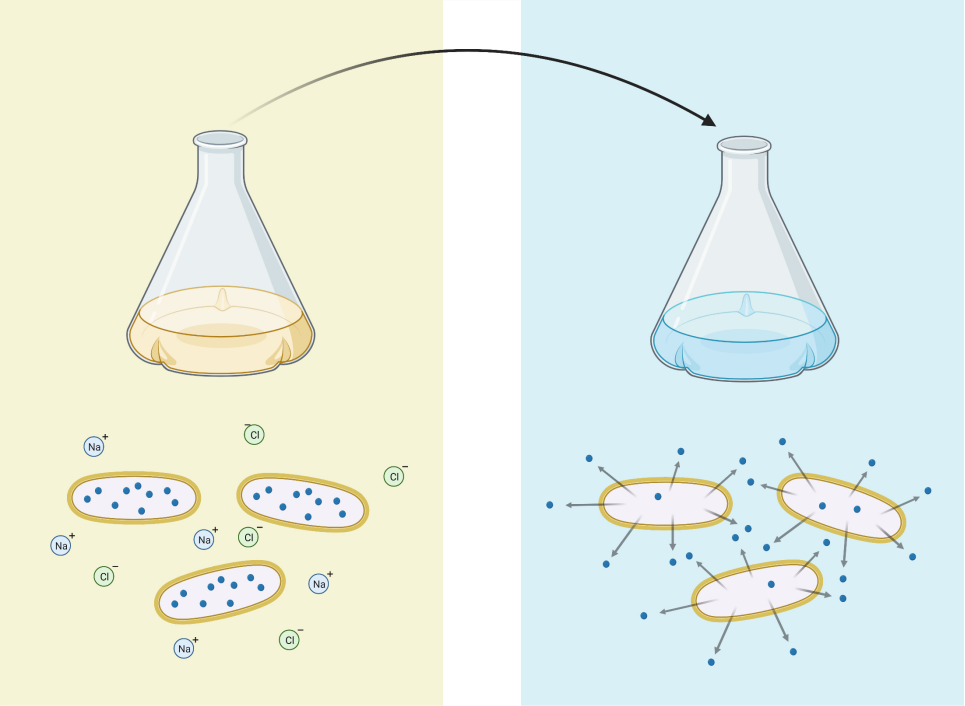

Figure 3.7: Illustration of the osmotic shock down concept. The cells are transferred from shake flasks with cultivation medium to shake flasks with equal volume of water. To balance the downshift of osmotic pressure, the intracellular compounds should be secreted from the cells to prevent osmotic lysis. The illustration was created with BioRender.com

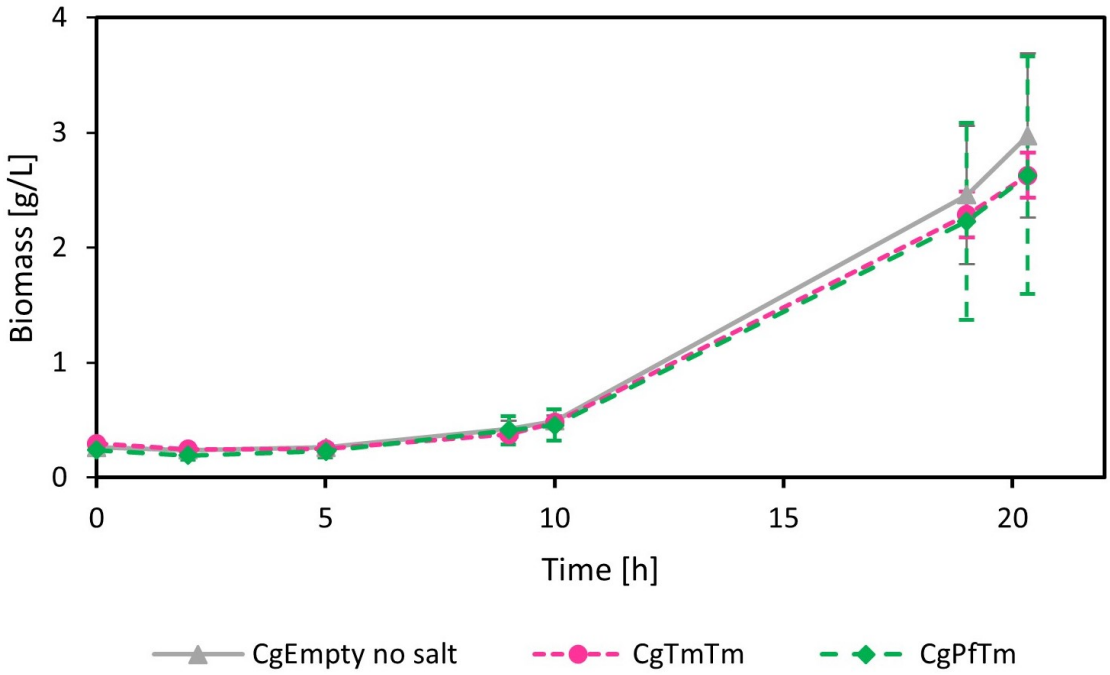

Figure 3.8: Growth curves from the shake flask fermentation in minimal medium supplemented with 0.5 M NaCl at 30°C, where the average biomass of the different strains are plotted against the fermentation time. When possible, average and standard deviation are shown.

Table 3.3: Results from the shake flask fermentation in minimal medium supplemented with 0.5 M NaCl at 30°C. The values show the average growth rate, final biomass and biomass yield. Average and standard deviation are shown. The final biomasses were calculated before the carbon source was depleted.

Strain Name	**Growth rate [h^{-1}]**	**Final Biomass [g/L]**
CgEmpty	0.17 ± 0.01	2.97 ± 0.71
CgTmTm	0.17 ± 0.00	2.63 ± 0.20
CgPfTm	0.15 ± 0.00	2.63 ± 1.03

Samples were taken of the cultivation when the fermentation was ended, directly after the osmotic shock down was started, and after 2, 4, and 72 hours (3 days) within the osmotic shock down process. The supernatant of the samples was analyzed using HPLC, however, due to the lack of commercially available DIP, the peaks could not be elucidated in this thesis. The HPLC results of the samples taken before the cells were exposed to the osmotic down-shift, showed peaks at the retention time of 7.1 min and 19.9 min. After the osmotic shock down, only peaks at the retention time of 19.9 min were present. The peaks were highest before the down-shift, and decreased drastically directly after, as seen in illustration a) Figure 3.9. Directly after the initial drop in peak height, all strains showed a sharp increase as a function of time, before ending with a small increasing slope. The slope of the increase in peak heights during the three first time-points for strain CgEmpty, CgTmTm, and CgPfTm, was 0.11 ± 0.06, 0.28 ± 0.13, and 0.20 ± 0.07, respectively. The total change in height at retention time 19.9 min after the osmotic shock down for CgEmpty, CgTmTm, and CgPfTm were 1.4 ± 0.4, 1.9 ± 0.4, and 1.9 ± 0.3, respectively. Here it was speculated that the compound with theretention time 19.9 min could be DIP, or could be related to the biosynthesis of DIP since the HPLC showed its accumulation during the osmotic shock down process, especially for the strain CgTmTm. Furthermore, such compound shares the retention time with a native compound since it was also observed in the strain CgEmpty. It was suggested the native compatible solute trehalose as it has a similar chemical structure, however that could not be confirmed via HPLC analyses (data not shown). The slopes and the changes in peak height are listed in Table 3.4. All HPLC values represented in Figure 3.9 are listed in Table C.6, found in Appendix C.

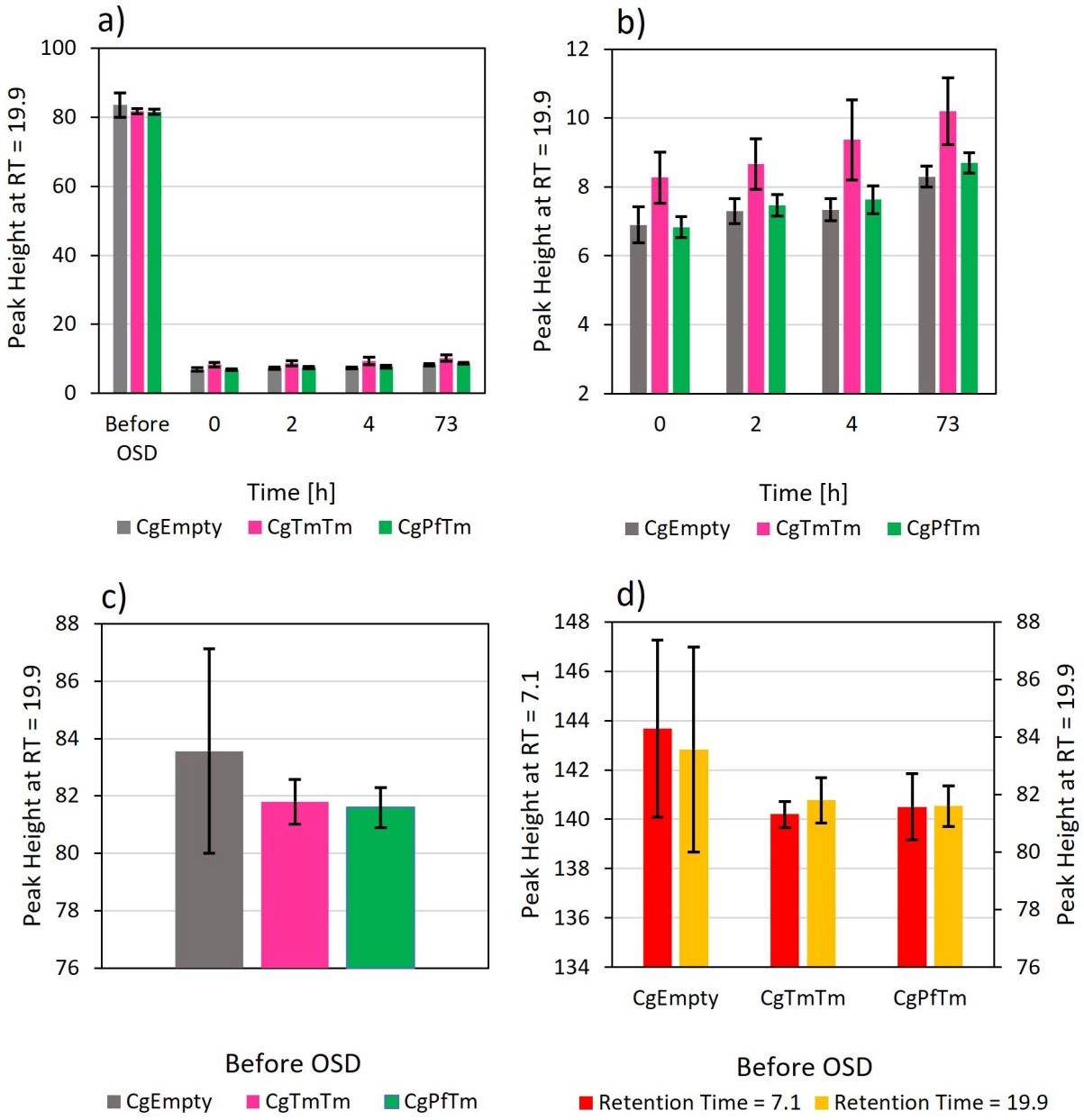

Figure 3.9: Graphs showing the peak heights of the HPLC analysis, as functions of time. The samples were taken during the shake flask fermentation in minimal media supplemented with 0.5 M NaCl at 30°C, and during the osmotic shock down process. Illustration a) shows the peak heights at the retention time of 19.9 min both after the fermentation, and during the osmotic shock down at the times 0, 2, 4 and 72 hours (3 days). Illustration b) and c) shows the peaks at retention time of 19.9 min after and before the osmotic shock down, respectively. Illustration d) shows the peak heights at the retention times of 7.1 min and 10.9 min, before the down-shift. Average and standard deviation values are shown.

Table 3.4: The results are based on peak heights at the retention time of 19.9 min from the HPLC analysis of the shake flask fermentation, coupled with an osmotic shock down. The slopes are from the increase in peak height during the three first time-points after the osmotic shock down where performed. The Δ peak heights are the total change seen after the osmotic down-shift. Average and standard deviation values are shown.

Strain Name	Slope	Δ Peak Height
CgEmpty	0.11 ± 0.06	1.4 ± 0.4
CgTmTm	0.28 ± 0.13	1.9 ± 0.4
CgPfTm	0.20 ± 0.07	1.9 ± 0.3

3.3 Scaling-up the Osmotic Shock Down Process in Lab-scale Bioreactor

Due to CgTmTm showing most promising growth behavior during earlier experiments, the strain was used for the scale-up in a bench-top bioreactor with 500 mL working volume. The fermentation was performed in minimal medium supplemented with 0.5 M NaCl at 30°C, and with 2 % glucose as sole carbon source. After the fermentation, the cells were centrifuged and washed with CGXII salt solution, before being resuspended in MilliQ water until the volume equaled the volume of the culture from which the pellets were separated. The osmotic shock down process was performed in an identical bioreactor. An illustration of the osmotic shock down concept is shown in Figure 3.10. As previously explained, during a fermentation with NaCl the cells should accumulate intracellular compounds, which should be secreted when transferred to water due to mechanosensitive channels.

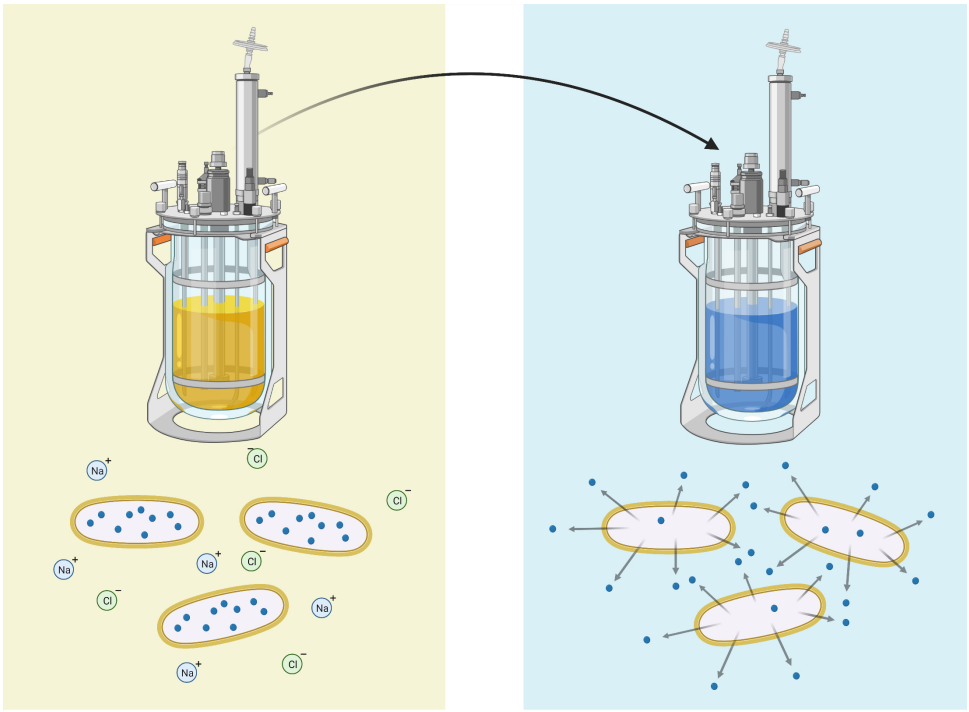

Figure 3.10: Illustration of the osmotic shock down concept. The cells are transferred from a bioreactor with minimal medium supplemented with 0.5 M NaCl, to a bioreactor with water. To balance the downshift of osmotic pressure, the intracellular compounds should be secreted from the cells to prevent osmotic lysis. The illustration was created with BioRender.com

Throughout the fermentation, samples were taken for biomass measurements, and for calculation of glucose concentration and identification of secreted compounds, using HPLC. The fermentation lasted 26 h before the carbon source was depleted. The decrease in biomass and stirring indicates the depletion, and correlates with the glucose concentrations calculated from the HPLC analyses. The biomass and glucose concentrations is plotted in the same graph as functions of time, shown in Figure 3.11. The stirring RPMs and the pO_2 is plotted in the same graph as functions of time, shown in Figure 3.12. The CgTmTm strain grew with a growth rate of 0.16 h^{-1}, a final biomass of 9.60 g/L and a biomass yield of 0.48 g/g. The growth values are listed in Table 3.5. The OD600 measurements used to make the growth curve are listed in Table C.4, found in Appendix C.

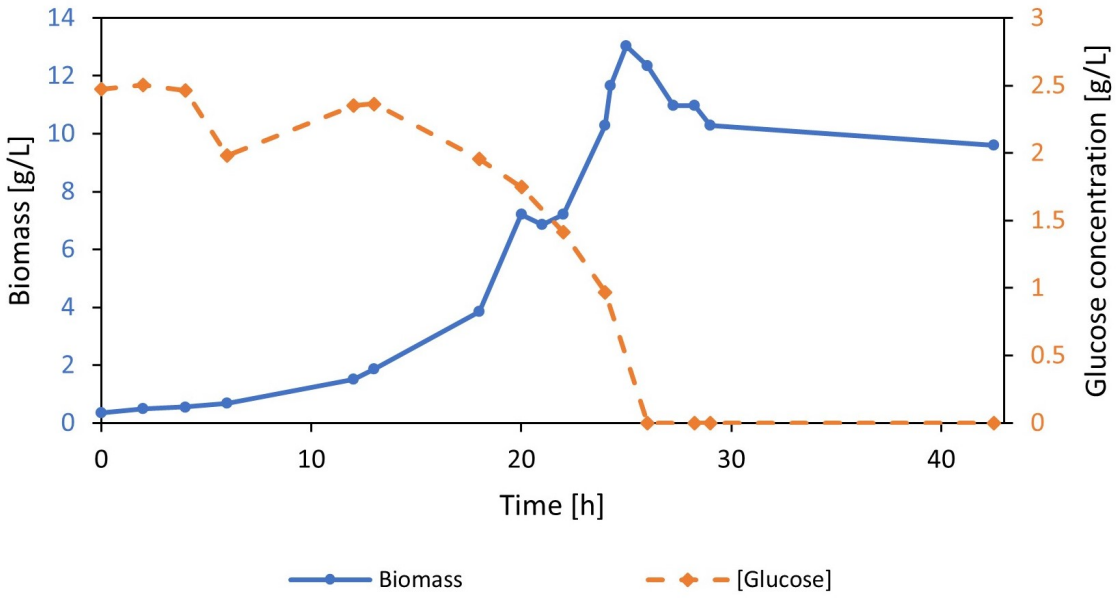

Figure 3.11: Graph showing the biomass and glucose consecration during the bench-top bioreactor fermentation of CgTmTm in minimal medium supplemented with 0.5 M NaCl at 30°C.

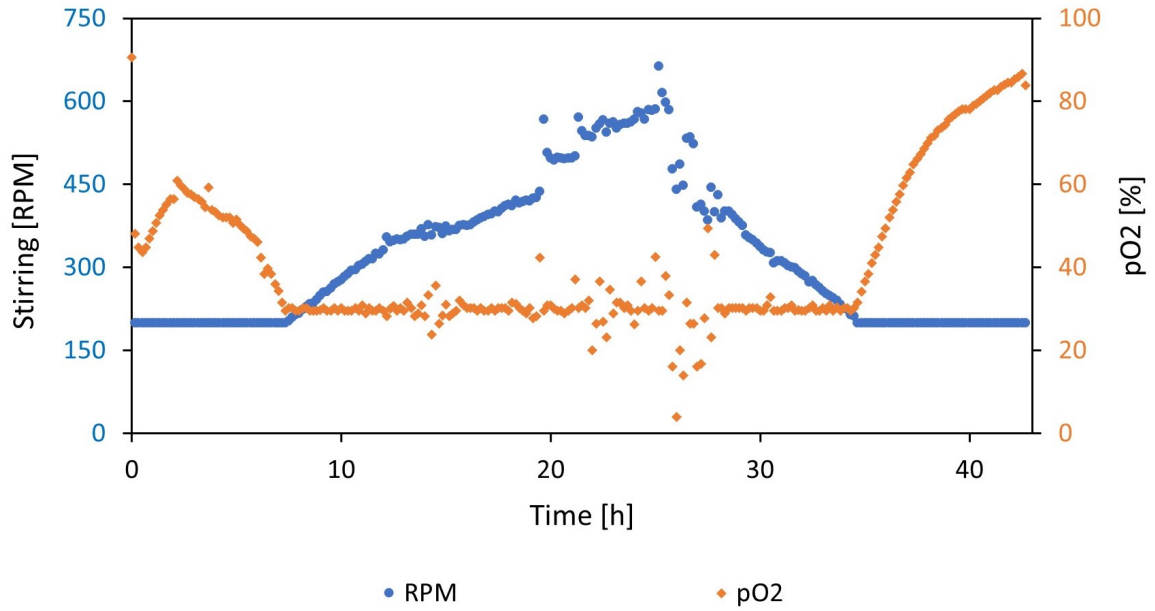

Figure 3.12: Graph showing the stirring power and pO_2 during the bench-top bioreactor fermentation of CgTmTm in minimal medium supplemented with 0.5 M NaCl at 30°C.

Table 3.5: Results from the bench-top bioreactor fermentation of CgTmTm in minimal medium supplemented with 0.5 M NaCl at 30°C. The values show the growth rate, final biomass, and biomass yield. The yield was calculated based on 20 g/L glucose as sole carbon source.

Strain Name	**Growth rate [h^{-1}]**	**Final Biomass [g/L]**	**Biomass Yield [g/g]**
CgTmTm	0.16	9.60	0.48

Excluding the peaks identified as glucose, HPLC peaks with the retention time of 7.1 min and 8.8 min were detected both during the fermentation and during the osmotic shock down process. In addition, peaks with a retention time of 19.9 min appeared after the osmotic down-shift. The heights of the peaks are presented as a function of time in Figure 3.13, where illustration a) shows the heights of all peaks from the initial inoculation, to the end of the osmotic shock down. The osmotic down-shift was performed after 43 hours, followed by a drastic fall in all peak heights. The peaks at the retention time of 7.1 min showed a relatively stable peak height before disappearing

as the cells were transferred from the medium to water. The peaks at the retention time of 8.8 min are first seen after six hours into the fermentation, and stagnate after 37 hours. When the biomass is transferred to water, the peak height drops drastically. The first hour after the osmotic down-shift, the peak heights had a sharper increase, before stagnating at a lower but increasing slope. After the osmotic shock down, peaks at the retention time of 19.9 min appeared. The peaks were a little higher than those at the retention time of 8.8 min, as well as showing a similar pattern. To easier see the differences in peak heights, two additionally graphs were created, showing the peaks before and after the osmotic down-shift as seen in illustration b) and c), respectively (Figure 3.13).

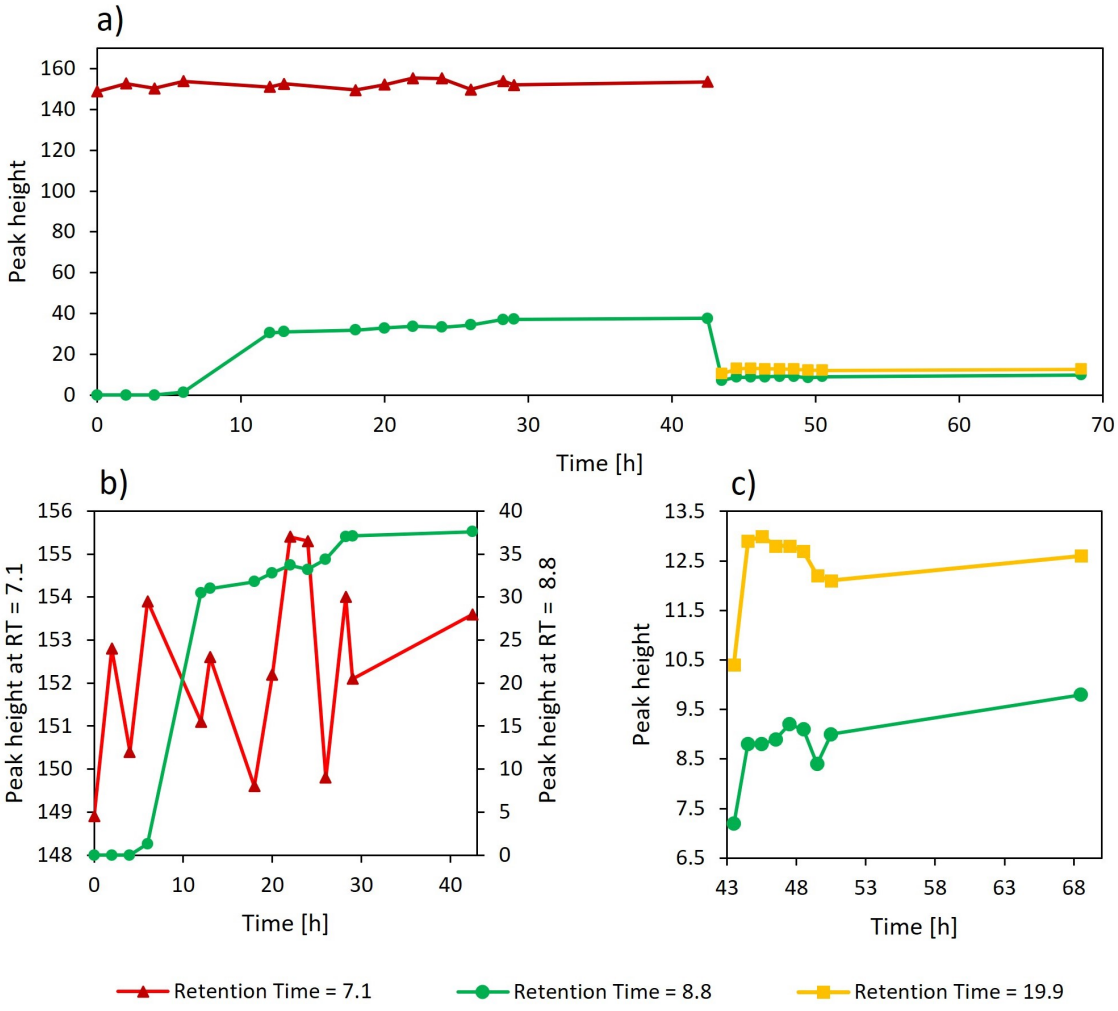

Figure 3.13: Graphs showing the peak heights from the HPLC analysis, as a function of time. The samples were taken during the bench-top bioreactor fermentation with the strain CgTmTm in minimal medium supplemented with 0.5 M NaCl at 30°C, and during the osmotic shock down process in an identical bioreactor. Illustration a) shows the peak heights at the retention time of 7.1 min, 8.8 min and 19.9 min during both the fermentation, and the osmotic shock down process. Illustration b) and c) shows the peaks during the fermentation, and the osmotic shock down, individually.

4 Discussion and Future Work

The compatible solute DIP is strictly found in hyperthermophilic organisms, which accumulate the compound in response to both osmotic and thermal stress[14]. The molecule represents an interesting product for microbial production due to the attributes desired in the pharmaceutical and cosmetic industries. Moreover, the production of DIP has yet to be commercialized, and the knowledge of its production is more restricted compared to other compatible solutes like ectoine or trehalose, whose production has been intensely exploited.

The founding literature describing the DIP synthesis pathway depict its stereochemical configuration as di-*myo*-1,1'-inositol-phosphate (Illustration a) Figure 1.7)[39]. Later studies have suggested that the designation di-*myo*-inositol-1,3'-phosphate should be used, as NMR analysis and carbon labeling of DIP extract from organisms such as *A. fulgidus*, *P. furiosus*, and *T. maritima* have this conformation[41]. The configuration of proline has been shown to affect its role as a compatible solute, where D-proline did not have the same osmoprotectant abilities as L-proline[43]. This gives reason to further investigate the stereochemical configuration of cellular synthesized DIP. Other methods to study this type of stereochemical configuration could be mass spectroscopy (MS), and gas chromatography (GC).

The microbial workhorse *C. glutamicum* have developed different strategies to combat osmotic stress, including the accumulation of compatible solutes. *C. glutamicum* can synthesize native compatible solutes such as L-proline, trehalose, and glutamine, as well as import others such as glycine, betaine, or ectoine[49][55][35]. Moreover, *C. glutamicum* has also been genetically engineered for the production of non-native compatible solutes such as ectoine, L-pipecolic acid, or mannosylglycerate[32][35][49]. When overexpressing the ectoine biosynthetic operon *ectABC* from *Chromohalobacter salexigens*, *C. glutamicum* reached an ectoine titer of 22 g/L and a product yield of 0.16 g/g, in a glucose fed-batch bioreactor fermentation[35]. When overexpressing the native *manA* gene, and the heterologous *manD* gene from *Dehalococcoides mccartyi*, *C. glutamicum* achieved a mannosylglycerate accumulation of 329 mM from glucose as carbon source[49]. When engineered for the production of L-pipecolic acid by overexpressing L-lysine 6-dehydrogenase from *Silicibacter pomeroyi* and the native

pyrroline 5-carboxylate reductase, as well as deletion of the native L-lysine export gene, *C. glutamicum* achieved a L-pipecolic acid titer of 14.4 g/L, and a product yield of 0.20 g/g. This was achieved in a glucose/sucrose based fed-batch fermentation[34]. *C. glutamicum* has also been engineered for the production of L-pipecolic acid under osmotic stress supplementing 200 mM of NaCl[32]. L-pipecolic acid has a very similar chemical structure as L-proline, which is a native compatible solute in *C. glutamicum*, and was shown to have a partial benefit to the cells during growth under osmotic pressure. Moreover, it was shown that an osmotic shock down increased the secretion of L-pipecolic acid apart from other native compatible solutes. Thus, there is a reason to think that *C. glutamicum* will secrete the intracellular accumulation of compatible solutes like DIP if subjected to an osmotic shock down, and could be a candidate for further establishment of a bacterial milking process. Ectoine is a compatible solute already commercially sold, and is produced using such process[44]. The process utilizes the extremophile *Halomonas elongata* in high-salinity fermentation, but drawbacks such as equipment corrosion, difficult contamination detection, and longer upstream processes constitute the desire for easier systems[48]. The use of mesophiles such as *C. glutamicum* offers an improved system for extremolyte productions, thus substantiating the relevance of this study.

In this work, *C. glutamicum* ATCC 13032 wild-type was genetically engineered for heterologous expression of the DIP biosynthesis pathway genes. For this purpose, the DIP operon genes expressing the enzymatic activities of IPS, IPCT, and DIPPS were cloned into the shuttle vector pVWEx1, while the gene expressing IMP was cloned into the shuttle vector pECx99a. The genes from the bacterium *T. maritima* and the archaeon *P. furiosus* were used to create four strains containing different combinations of the vectors needed to complete the DIP biosynthesis pathway (Table 2.2). The strains CgTmTm and CgPfTm contain the DIP operon from the bacterium *T. maritima*, while CgPfPf and CgTmPf contain the DIP operon from archeon *P. furiosus*. Accumulation of DIP has been found in both thermophilic Archaea and Bacteria, where homologous genes encoding the IPCT and DIPPS activities have been present in all related organisms with sequenced genome[41]. The activation energy for the key enzymatic activities of IPS, IMP, and DIPPS measured at 85°C in crud protein extract prepared from *Methanococcus igneus*, have been found to be 60-70 kJ/mol, 54 kJ/mol, and 120

kJ/mol, respectively[6]. As the presence of DIPPS is required for DIP biosynthesis, and as it needs higher activation energy, it is reasonable to assume that the enzymatic activity of DIPPS could be the bottleneck of the DIP biosynthesis. DIP is found in hyperthermophiles, meaning that the organisms and the DIP biosynthesis pathways are distinctively adapted for optimum growth and functions above a temperature of 80°C. For *T. maritima*, the optimum growth temperature is 80°C, and for *P. furiosus* it is at around 100°C. In both the BioLector fermentation in regular minimal medium at 30°C, and the BioLector fermentation in minimal medium supplemented with 0.5 M NaCl at 30°C, the strains showed similar growth behavior in regards to the lag phases. The strains expressing the IPS, IPCT, and DIPPS from *P. furiosus* had longer lag growth phases, than the strains with the same activities from *T. maritima*. This additionally correlates to the temperature dependency of the enzymatic activity of DIPPS, which has high activation energy. The suboptimal temperature could lead to the key enzymes not folding correctly, or the production of uncompleted amino acid sequences during translation. At lower temperatures, the enzymatic activity of DIPPS decreases. The intermediate L-*myo*-inositol-phosphate could then be hydrolyzed into *myo*-inositol, a precursor in the synthesis of the membrane phospholipid phosphatidyl-*myo*-inositol found in *C. glutamicum*[6] [24]. This could indicate the reason for the longer lag phase for the strains with DIP operon from *P. furiosus*, compared to the strains with the operon from *T. maritima*, is due to *P. furiosus* having a higher optimum growth temperature. Additionally, the IPCT and DIPPS activities in *P. furiosus* is fused in one gene, while the genes of *T. maritima* are found separated and consecutive. Due to belonging to the domain Bacteria, *T. maritima* is likely more evolved than the archeon *P. furiosus*, thus has had more time to optimize its genes needed to withstand abiotic stresses. As *T. maritima* is both more evolved, and more closely related to the host strain *C. glutamicum* than *P. furiosus*, it is plausible that the DIP biosynthesis genes are expressed more efficiently and correctly, leading to less wrongly folded proteins and uncompleted amino acid sequences. Production of misfolded proteins/inclusion bodies, which is likely in this case, translates to a carbon loss and could impact the growth as in, for instance, increasing the lag phase. The redirection of the carbon flow for the production of a heterologous protein also explains the lower growth rates and final biomass, which was expected and indicates the presence of production.

The constructed strains were tested under osmotic stress, and BioLector fermentations supplemented with 0.5 M, 1.0 M, and 1.5 M NaCl were performed. The overexpression of the DIP biosynthesis pathway in *C. glutamicum* resulted in higher final biomass under osmotic stress of 0.5 M NaCl for all the recombinant strains compared to the control strain CgEmpty (Figure 3.4). However, the only strains with higher growth rates than the control strain were CgTmTm and CgPfTm (Figure 3.4). This could also suggest that the DIP operon from *T. maritima* is more effective as discussed earlier. Under the fermentation with supplemented 1.0 M NaCl, only one parallel from the strains CgTmTm, CgPfTm and CgTmPf grew (Figure 3.5). The control strain grown without supplemented NaCl, had a growth rate of 0.21 ± 0.01 h^{-1} and a final biomass of 5.37 ± 0.20 g/L. Compared to the two previous BioLector fermentations of the control strain CgEmpty at 30°C, the significantly lower growth rate and final biomass indicate that the experiment was compromised due to unidentified technical errors. When looking at the results qualitatively, the growth of the single parallels can stem from random mutations or differences in the separated parallel colonies, and would be interesting to further investigate. The CgTmTm had the best growth rate of 0.03 h^{-1}, and final biomass of 2.40 g/L. This is very poor growth, but the fact that CgTmTm was able to survive high osmotic stress, indicates that osmoprotectants are being produced. The growth behavior of CgTmTm in 1.0 M NaCl shows a very long lag phase, and enters the exponential phase after a cultivation time of 100 h (Figure 3.5). Due to this extensive cultivation time, the fermentation was ended before the growth entered the stationary phase, thus leaving the final biomass not necessarily representative of the possible growth. The extensive lag phase can be due to *C. glutamicum* needing time to accumulate a sufficient concentration of compatible solutes to allow growth. Since the control strain supplemented with 1 M NaCl had no growth, the accumulated compatible solutes in CgTmTm are suspected to be DIP.

Hyperthermophilic organisms such as *T. maritima* and *P. furiosus* grow at astonishing high temperatures. However, it has been found that purified enzymes of such hyperthermophiles generally are unstable at the optimum growth temperature of the organism from which they are extracted[37]. This suggests the need for thermoprotectant compounds, and that hyperthermophiles either synthesize or import the molecules they need. Both *T. maritima* and *P. furiosus* accumulate DIP in

response to increasing temperature, and DIP is therefore thought to be associated with thermoprotection[29][30][39]. When the strains constructed in this study were cultivated in the BioLector at the supraoptimal temperature of 40°C, only the control strain CgEmpty grew (Figure 3.2). The growth rate and final biomass were 0.10 ± 0.02 h^{-1}, and 0.86 ± 0.17 g/L, respectively. The DIP biosynthesis pathway uses L-glucose-6-phosphate as the initial precursor[14][41]. This intermediate connects to the glycolysis, a central metabolic pathway in *C. glutamicum*[25][16]. Redirecting the carbon flux away from this central carbon metabolism leaves less carbon sources for energy and biomass production. This could explain why only the control strain grew, and could indicate that the production of DIP could be metabolically expensive for the cells. The lack of growth at 40°C for any of the genetically modified strain, show that the overexpressing of the DIP biosynthesis pathway genes did not contribute to thermal protection under the conditions tested here. As discussed earlier, the enzymatic activity of DIPPS or IPCT is suspected to be the bottleneck for the DIP biosynthesis pathway. Moreover, the folding and function of the key enzymes, natively found in hyperthermophiles, are temperature dependent, where the activation energy of DIPPS is found to be 120 kJ/mol. In this work, it was seen that the amount of DIP produced during the fermentation at 40°C is not sufficient enough to potentially have an thermoprotectant effect, and to counteract the negative impact heterologous production and supraoptimal temperature have on the expression host *C. glutamicum*.

Following the initial screening, a shake flask fermentation with the strains CgTmTm, CgPfTm, and CgEmpty as a control, were performed in 50 mL minimal medium supplemented with 0.5 M NaCl at 30°C. The strains were chosen due to having the highest growth rates during the BioLector fermentation at 30°C, and the BioLector fermentation supplemented with 0.5 M NaCl. In addition, the strains exhibited the shortest lag phases, and both had parallels in the BioLector fermentation supplemented with 1.0 M NaCl, that grew. When produced in *Rhodothermus* spp., the concentration of the compatible solute α-mannosylglycerate has been found to increase during the exponential phase, before abruptly decreasing when the cells entered the stationary phase[50]. DIP is a compound related to growth, and both DIP and α-mannosylglycerate are negatively charged compatible solutes[41][38]. Due to these similarities, the shake flask experiment was ended in what was believed to be

the late exponential phase for the extraction of DIP, as high intracellular concentrations were desired to test the potential of the osmotic shock down process.

For the extraction of DIP, and its detection using HPLC, both the shake flask and the lab-scale bioreactor fermentations were coupled with an osmotic shock down. Unfortunately, DIP is not commercially available. Moreover, when seeking a DIP sample, the German company Bitop AG was contacted since it produces and commercialized compatible solutes like ectoine. However, no positive response was obtained. Hence, the identification of DIP via HPLC was not possible during this research work. Regardless, the samples were analyzed using HPLC to gain qualitative insights.

During the shake flask fermentation supplemented with 0.5 M NaCl at 30°C, samples were taken when the fermentation was ended, directly after the osmotic shock down had started, and after 2, 4, and 72 hours (3 days). The HPLC showed peaks at the retention times of 7.1 min and of 19.9 min. After the osmotic shock down, only the peaks at the retention time of 19.9 min remained, suggesting that the carbohydrate-like molecule with the retention time of 7.1 min is not secreted from the cells during osmotic down-shifts. Before the osmotic shock down, the control strain CgEmpty, grown in minimal medium supplemented with 0.5 M NaCl, had the highest peak at the retention time of 19.9 min, while CgTmTm and CgPfTm showed similar but smaller peak heights (Figure 3.9 c)). When being subjected to an osmotic shock down, the secretion of compatible solutes generally goes through two phases; first a rapid release, before a slow leakage of the remaining content[3]. After the osmotic shock down, all stains had a decrease in peak heights before a sharper increase, followed by a slower increase. The slopes of this sharper increase for CgEmpty, CgTmTm and CgPfTm are listed in Table 3.4, and were 0.11 $\pm$ 0.06, 0.28 $\pm$ 0.13, and 0.20 $\pm$ 0.07, respectively. Despite the overall small changes, the trend indicates a release of carbohydrate-presenting molecules. One explanation could be that the retention time of 19.9 min is shared between both DIP and a native osmoprotectant. If the native compound has active channels, this would explain the high peaks at the end of the fermentation, as the strains would produce and secret the unknown compatible solute during the fermentation. This fits with CgEmpty having the highest peak before the

osmotic shock down, as DIP being produced in the modified strains would result in less osmotic stress, thus reducing the need for native osmo-protection. Due to DIP not being native to *C. glutamicum* wild-type, no active channels should be present to secret DIP without an osmotic shock down. When subjected to an osmotic down-shift, mechanosensitive channels should secrete the remaining compatible solutes preventing cell bursting[48] [26]. This indicates that the peaks at the retention time of 7.1 min are not DIP, as the peaks are not seen after the osmotic down-shift. After the osmotic shock down, the increase in peak heights at the retention time of 19.9 min for CgEmpty, CgTmTm, and CgPfTm were 1.4 ± 0.4, 1.9 ± 0.4 and 1.9 ± 0.3, respectively. The difference between the control strain and the constructed stains could represent the secreted DIP.

The samples taken during the bench-top bioreactor fermentation, and the osmotic shock down process, were analyzed using the HPLC, and the results are illustrated in Figure 3.13. The HPLC analysis showed peaks at the retention times of 7.1 min, 8.8 min, and 19.9 min. Excluding the retention time of 8.8 min, this correlates to peaks found in the HPLC analysis for the shake flask experiment. After the osmotic shock down, only the peaks at the retention time of 8.8 min and 19.9 min remained, substantiating that the carbohydrate-like molecule with the retention time of 7.1 min is not secreted from the cells during osmotic down-shifts. As seen in illustration a) in Figure 3.13, the compound with the retention time of 8.8 min first appeared after 6 h, and stagnates after 28 h. This is around when the carbon source was depleted, making the compound look related to the growth. After the CgTmTm was subjected to the osmotic shock down, the peak height at the retention time of 8.8 min decreased substantially. After the down-shift, the peak heights increased sharply, before dipping shortly, followed by a slower increasing slope. Due to the increase in peak height after the osmotic shock down, the compound is believed to be a compatible solute. As it is very unlikely that *C. glutamicum* possesses an active transport system for a non-native product as DIP, it is assumed to be a native compatible solute as L-proline or trehalose[49] [55] [35]. The compound with the retention time of 19.9 min shared the pattern described for the peaks with the retention time of 8.8 min, but first appeared after the down-shift. The secretion of DIP requires an osmotic down-shift, indicating that the compound with the retention time of 19.9 min could be DIP. Comparing the

HPLC results from the bioreactors with the results from the shake flask fermentation, the suspicion of DIP having the retention time of 19.9 min is strengthened.

Due to the lack of standards, neither the identity of the peaks, nor the concentration of the product can be determined. Moreover, there were no methods to determine the extent to which the compatible solutes were secreted compared to how much was left inside the cells. Trehalose is the only native compatible solute of *C. glutamicum* wild-type with a similar carbohydrate structure, and thus most likely to overlap with the potential retention time of DIP, or being identified as the compound with the retention time of 8.8 min[54][49][55][35]. L-Lactate is another carbohydrate produced by *C. glutamicum* wild-type, and is prominently induced during the transition between late exponential phase and stationary growth phase, although not a compatible solute[51]. Standards of trehalose and L-lactate were used for HPLC analyses to compare the peaks believed to contain DIP, but due to technical fluctuations of the HPLC system, the data was inconclusive.

4.1 Further Work

Firstly, the identification of DIP should be confirmed. If DIP standards are obtained, additional HPLC analysis could be performed to cross-reference the results from this work. Another possibility for confirming the presents of DIP could be mass spectroscopy (MS), nuclear magnetic resonance (NMR), and gas chromatography (GC). Due to the high optimal temperatures of *T. maritima* and *P. furiosus*, the enzymatic activities of the proteins could be low due to suboptimal temperature. If DIP is identified, the purification and quantification of the DIP biosynthesis enzymatic activities could be performed. Lastly, if strains based on this work show improved results, up-scaling to larger bioreactors and/or optimizing the osmotic shock down process would be of great interest to achieve industrially competent production values.

5 Conclusion

In this work, *C. glutamicum* ATCC 13032 was genetically engineered for heterologous expression of the DIP biosynthesis pathway genes. This was achieved by combining genes from the hyperthermophiles *T. maritima* and *P. furiosus*. The strains expressing the genes encoding for the enzymatic activities IPCT and DIPPS from the bacterium *T. maritima*, showed very promising results with regards to DIP production using an osmotic shock down approach, despite the fact of lacking direct confirmation of DIP formation. Finally, the osmotic shock down process was successfully adapted and tested with the best-performing strain CgTmTm in lab-scale bioreactors, proving the feasibility of this bioprocesses and laying the cornerstone for the production of unconventional compatible solutes with *C. glutamicum*.

References

[1] Abe, S., Takayama, K.-I. and Kinoshita, S. [1967]. Taxonomical studies on glutamic acid-producing bacteria, *The Journal of General and Applied Microbiology* **13**(3): 279–301.

[2] Antón, J. [2011]. Compatible Solute, *Encyclopedia of Astrobiology*, Springer Berlin Heidelberg, Berlin, Heidelberg, pp. 351–352.

[3] Bialecka-Fornal, M., Lee, H. J. and Phillips, R. [2015]. The rate of osmotic downshock determines the survival probability of bacterial mechanosensitive channel mutants., *Journal of bacteriology* **197**(1): 231–7.

[4] Botta, C., Di Giorgio, C., Sabatier, A.-S. and De Méo, M. [2008]. Genotoxicity of visible light (400–800nm) and photoprotection assessment of ectoin, l-ergothioneine and mannitol and four sunscreens, *Journal of Photochemistry and Photobiology B: Biology* **91**(1): 24–34.

[5] Buenger, J. and Driller, H. [2004]. Ectoin: An Effective Natural Substance to Prevent UVA-Induced Premature Photoaging, *Skin Pharmacology and Physiology* **17**(5): 232–237.

[6] Chen, L., Spiliotis, E. T. and Roberts, M. F. [1998]. Biosynthesis of Di-*myo*-Inositol-1,1'-Phosphate, a Novel Osmolyte in Hyperthermophilic Archaea, *Journal of Bacteriology* **180**(15): 3785–3792.

[7] Czech, L., Hermann, L., Stöveken, N., Richter, A., Höppner, A., Smits, S., Heider, J. and Bremer, E. [2018]. Role of the Extremolytes Ectoine and Hydroxyectoine as Stress Protectants and Nutrients: Genetics, Phylogenomics, Biochemistry, and Structural Analysis, *Genes* **9**(4): 177.

[8] da Costa, M. S., Santos, H. and Galinski, E. A. [1998]. An overview of the role and diversity of compatible solutes in Bacteria and Archaea, pp. 117–153.

[9] Empadinhas, N. and da Costa, M. S. [2008]. Osmoadaptation mechanisms in prokaryotes: distribution of compatible solutes., *International microbiology : the official journal of the Spanish Society for Microbiology* **11**(3): 151–61.

[10] Esteves, A. M., Chandrayan, S. K., McTernan, P. M., Borges, N., Adams, M. W. W.

and Santos, H. [2014]. Mannosylglycerate and Di-*myo*-Inositol Phosphate Have Interchangeable Roles during Adaptation of *Pyrococcus furiosus* to Heat Stress, *Applied and Environmental Microbiology* **80**(14): 4226–4233.

[11] Fedotova, M. V. [2019]. Compatible osmolytes - bioprotectants: Is there a common link between their hydration and their protective action under abiotic stresses?, *Journal of Molecular Liquids* **292**: 111339.

[12] Galinski, E. A. and Herzog, R. M. [1990]. The role of trehalose as a substitute for nitrogen-containing compatible solutes (*Ectothiorhodospira halochloris*), *Archives of Microbiology* **153**(6): 607–613.

[13] Garcia-Estepa, R., Argandona, M., Reina-Bueno, M., Capote, N., Iglesias-Guerra, F., Nieto, J. J. and Vargas, C. [2006]. The *ectD* Gene, Which Is Involved in the Synthesis of the Compatible Solute Hydroxyectoine, Is Essential for Thermoprotection of the Halophilic Bacterium *Chromohalobacter salexigens*, *Journal of Bacteriology* **188**(11): 3774–3784.

[14] Gonçalves, L. G., Borges, N., Serra, F., Fernandes, P. L., Dopazo, H. and Santos, H. [2012]. Evolution of the biosynthesis of di-*myo*-inositol phosphate, a marker of adaptation to hot marine environments, *Environmental Microbiology* **14**(3): 691–701.

[15] Görke, B. and Stülke, J. [2008]. Carbon catabolite repression in bacteria: many ways to make the most out of nutrients, *Nature Reviews Microbiology* **6**(8): 613–624.

[16] Graf, R., Anzali, S., Buenger, J., Pfluecker, F. and Driller, H. [2008]. The multifunctional role of ectoine as a natural cell protectant, *Clinics in Dermatology* **26**(4): 326–333.

[17] Han, J., Gao, Q.-X., Zhang, Y.-G., Li, L., Mohamad, O. A. A., Rao, M. P. N., Xiao, M., Hozzein, W. N., Alkhalifah, D. H. M., Tao, Y. and Li, W.-J. [2018]. Transcriptomic and Ectoine Analysis of Halotolerant *Nocardiopsis gilva* YIM 90087T Under Salt Stress, *Frontiers in Microbiology* **9**.

[18] Hanahan, D. [1983]. Studies on transformation of *Escherichia coli* with plasmids, *Journal of Molecular Biology* **166**(4): 557–580.

[19] Hashimoto, S.-i. [2016]. Discovery and History of Amino Acid Fermentation, pp. 15–34.

[20] Henke, N. A., Peters-Wendisch, P. and Wendisch, V. F. [2017]. Carotenoid Production by *Corynebacterium*: The Workhorse of Industrial Amino Acid Production as Host for Production of a Broad Spectrum of C40 and C50 Carotenoids, *Carotenoids*, InTech.

[21] Jadhav, K., Kushwah, B. and Jadhav, I. [2018]. Insight into Compatible Solutes from Halophiles: Exploring Significant Applications in Biotechnology, *Microbial Bioprospecting for Sustainable Development*, Springer Singapore, Singapore, pp. 291–307.

[22] Kirchner, O. and Tauch, A. [2003]. Tools for genetic engineering in the amino acid-producing bacterium *Corynebacterium glutamicum*., *Journal of biotechnology* **104**(1-3): 287–99.

[23] Kirsch, F., Klähn, S. and Hagemann, M. [2019]. Salt-Regulated Accumulation of the Compatible Solutes Sucrose and Glucosylglycerol in *Cyanobacteria* and Its Biotechnological Potential, *Frontiers in Microbiology* **10**.

[24] Krings, E., Krumbach, K., Bathe, B., Kelle, R., Wendisch, V. F., Sahm, H. and Eggeling, L. [2006]. Characterization of *myo*-Inositol Utilization by *Corynebacterium glutamicum* : the Stimulon, Identification of Transporters, and Influence on L-Lysine Formation, *Journal of Bacteriology* **188**(23): 8054–8061.

[25] Kumari, A. [2018]. Glycolysis, *Sweet Biochemistry*, Elsevier, pp. 1–5.

[26] Kung, C., Martinac, B. and Sukharev, S. [2010]. Mechanosensitive Channels in Microbes, *Annual Review of Microbiology* **64**(1): 313–329.

[27] Latif, H., Lerman, J. A., Portnoy, V. A., Tarasova, Y., Nagarajan, H., Schrimpe-Rutledge, A. C., Smith, R. D., Adkins, J. N., Lee, D.-H., Qiu, Y. and Zengler, K. [2013]. The Genome Organization of *Thermotoga maritima* Reflects Its Lifestyle, *PLoS Genetics* **9**(4): e1003485.

[28] Liebl, W. [2006]. *Corynebacterium*–Nonmedical, *The Prokaryotes*, Springer New York, New York, NY, pp. 796–818.

[29] Martins, L. O., Carreto, L. S., Da Costa, M. S. and Santos, H. [1996]. New compatible solutes related to Di-*myo*-inositol-phosphate in members of the order *Thermotogales*, *Journal of Bacteriology* **178**(19): 5644–5651.

[30] Martins, L. O. and Santos, H. [1995]. Accumulation of Mannosylglycerate and Di-*myo*-Inositol-Phosphate by *Pyrococcus furiosus* in Response to Salinity and Temperature, *Applied and Environmental Microbiology* **61**(9): 3299–3303.

[31] Ohtake, S. and Wang, Y. J. [2011]. Trehalose: Current Use and Future Applications, *Journal of Pharmaceutical Sciences* **100**(6): 2020–2053.

[32] Pérez-García, F., Brito, L. F. and Wendisch, V. F. [2019]. Function of L-Pipecolic Acid as Compatible Solute in *Corynebacterium glutamicum* as Basis for Its Production Under Hyperosmolar Conditions, *Frontiers in Microbiology* **10**.

[33] Pérez-García, F., Burgardt, A., Kallman, D. R., Wendisch, V. F. and Bar, N. [2021]. Dynamic Co-Cultivation Process of *Corynebacterium glutamicum* Strains for the Fermentative Production of Riboflavin, *Fermentation* **7**(1): 11.

[34] Pérez-García, F., Max Risse, J., Friehs, K. and Wendisch, V. F. [2017]. Fermentative production of L-pipecolic acid from glucose and alternative carbon sources, *Biotechnology Journal* **12**(7): 1600646.

[35] Pérez-García, F., Ziert, C., Risse, J. M. and Wendisch, V. F. [2017]. Improved fermentative production of the compatible solute ectoine by *Corynebacterium glutamicum* from glucose and alternative carbon sources, *Journal of Biotechnology* **258**: 59–68.

[36] Peters-Wendisch, P. G., Schiel, B., Wendisch, V. F., Katsoulidis, E., Möckel, B., Sahm, H. and Eikmanns, B. J. [2001]. Pyruvate carboxylase is a major bottleneck for glutamate and lysine production by *Corynebacterium glutamicum*., *Journal of molecular microbiology and biotechnology* **3**(2): 295–300.

[37] Ramakrishnan, V., Verhagen, M. and Adams, M. [1997]. Characterization of Di-*myo*-Inositol-1,1(prm1)-Phosphate in the Hyperthermophilic Bacterium *Thermotoga maritima*, *Applied and Environmental Microbiology* **63**(1): 347–350.

[38] Roberts, M. F. [2005]. Organic compatible solutes of halotolerant and halophilic microorganisms, *Saline Systems* **1**(1): 5.

[39] Rodionov, D. A., Kurnasov, O. V., Stec, B., Wang, Y., Roberts, M. F. and Osterman, A. L. [2007]. Genomic identification and in vitro reconstitution of a complete biosynthetic pathway for the osmolyte di-*myo*-inositol-phosphate, *Proceedings of the National Academy of Sciences* **104**(11): 4279–4284.

[40] Rodrigues, M. V., Borges, N., Almeida, C. P., Lamosa, P. and Santos, H. [2009]. A Unique β-1,2-Mannosyltransferase of *Thermotoga maritima* That Uses Di-*myo*-Inositol Phosphate as the Mannosyl Acceptor, *Journal of Bacteriology* **191**(19): 6105–6115.

[41] Rodrigues, M. V., Borges, N., Henriques, M., Lamosa, P., Ventura, R., Fernandes, C., Empadinhas, N., Maycock, C., da Costa, M. S. and Santos, H. [2007]. Bifunctional CTP:Inositol-1-Phosphate Cytidylyltransferase/CDP-Inositol:Inositol-1-Phosphate Transferase, the Key Enzyme for Di-*myo*-Inositol-Phosphate Synthesis in Several (Hyper)thermophiles, *Journal of Bacteriology* **189**(15): 5405–5412.

[42] Santos, H. and da Costa, M. S. [2002]. Compatible solutes of organisms that live in hot saline environments, *Environmental Microbiology* **4**(9): 501–509.

[43] Sasaki, H., Takaki, A., Oshima, A., Ishida, A. and Nagata, S. [2007]. Comparison of the function of L- and D-proline as compatible solute in *Escherichia coli* K-12 under high osmolarity, *Annals of Microbiology* **57**(2): 265–268.

[44] Sauer, T. and Galinski, E. A. [1998]. Bacterial milking: A novel bioprocess for production of compatible solutes, *Biotechnology and Bioengineering* **57**(3): 306–313.

[45] Schnoor, M., Voß, P., Cullen, P., Böking, T., Galla, H.-J., Galinski, E. A. and Lorkowski, S. [2004]. Characterization of the synthetic compatible solute homoectoine as a potent PCR enhancer, *Biochemical and Biophysical Research Communications* **322**(3): 867–872.

[46] Schobert, B. and Tschesche, H. [1978]. Unusual solution properties of proline and

its interaction with proteins, *Biochimica et Biophysica Acta (BBA) - General Subjects* **541**(2): 270–277.

[47] Scholz, S., Sonnenbichler, J., Schäfer, W. and Hensel, R. [1992]. Di-*myo*-inositol-1, 1'-phosphate: A new inositol phosphate isolated from *Pyrococcus woesei*, *FEBS Letters* **306**(2-3): 239–242.

[48] Schubert, T., Maskow, T., Benndorf, D., Harms, H. and Breuer, U. [2007]. Continuous Synthesis and Excretion of the Compatible Solute Ectoine by a Transgenic, Nonhalophilic Bacterium, *Applied and Environmental Microbiology* **73**(10): 3343–3347.

[49] Schwentner, A., Neugebauer, H., Weinmann, S., Santos, H. and Eikmanns, B. J. [2021]. Exploring the Potential of *Corynebacterium glutamicum* to Produce the Compatible Solute Mannosylglycerate, *Frontiers in Bioengineering and Biotechnology* **9**.

[50] Silva, Z., Borges, N., Martins, L. O., Wait, R., da Costa, M. S. and Santos, H. [1999]. Combined effect of the growth temperature and salinity of the medium on the accumulation of compatible solutes by *Rhodothermus marinus* and *Rhodothermus obamensis*, *Extremophiles* **3**(2): 163–172.

[51] Toyoda, K. and Inui, M. [2021]. The *ldh*A Gene Encoding Fermentative l-Lactate Dehydrogenase in *Corynebacterium Glutamicum* Is Positively Regulated by the Global Regulator GlxR, *Microorganisms* **9**(3): 550.

[52] Van-Thuoc, D., Guzmán, H., Quillaguamán, J. and Hatti-Kaul, R. [2010]. High productivity of ectoines by *Halomonas boliviensis* using a combined two-step fed-batch culture and milking process, *Journal of Biotechnology* **147**(1): 46–51.

[53] Weinisch, L., Kühner, S., Roth, R., Grimm, M., Roth, T., Netz, D. J. A., Pierik, A. J. and Filker, S. [2018]. Identification of osmoadaptive strategies in the halophile, heterotrophic ciliate *Schmidingerothrix salinarum*., *PLoS biology* **16**(1): e2003892.

[54] Welsh, D. T. [2000]. Ecological significance of compatible solute accumulation by micro-organisms: from single cells to global climate, *FEMS Microbiology Reviews* **24**(3): 263–290.

[55] Wolf, A., Krämer, R. and Morbach, S. [2003]. Three pathways for trehalose metabolism in *Corynebacterium glutamicum* ATCC13032 and their significance in response to osmotic stress, *Molecular Microbiology* **49**(4): 1119–1134.

[56] Xiao, Z., Yang, S., Chen, J., Li, C., Zhou, C., Hong, P., Sun, S. and Qian, Z.-J. [2020]. Trehalose against UVB-induced skin photoaging by suppressing MMP expression and enhancing procollagen I synthesis in HaCaT cells, *Journal of Functional Foods* **74**: 104198.

A Recipes for Solutions Used in This Work

A.1 CGXII Salt Solution

The CGXII salt solution was prepared using the recipe showed in Table A.1. Before adding water, the pH was adjusted to 7.0 using 5 M KOH. After the preparation, the solution was sterilized using autoclavation.

Table A.1: Recipe for the CGXII salt solution.

Components	**Concentration**	**Units**
$(NH_4)_{2SO_4}$	10	g/L
KH_2PH_4	1	g/L
K_2HPO_4	1	g/L
UREA	5	g/L
MOPS	42	g/L
Ca-stock 1000X	1	mL/L
Mg-stock 1000X	1	mL/L
Fill up with deionized water until the final volume is reached		

A.2 Glucose 40% Solution

The glucose 40% solution was prepared using the recipe showed in Table A.2. After the preparation, the solution was sterilized using filtration.

Table A.2: Recipe for the Glucose 40% solution.

Component	**Concentration**	**[g/L]**
Glucose	400	
Fill up with deionized water until the final volume is reached		

A.3 Sorbitol Solution

The sorbitol solution was prepared using the recipe showed in Table A.3. After the preparation, the solution was sterilized using autoclavation.

Table A.3: Recipe for the sorbitol solution.

Component	**Concentration**	**[g/L]**
Sorbitol	455	
Fill up with deionized water until the final volume is reached		

A.4 Glycerin 89 % Solution

The glycerin 89% solution was prepared using the recipe showed in Table A.4. After the preparation, the solution was sterilized using autoclavation.

Table A.4: Recipe for the glycerin 89 % solution.

Components	**Concentration**	**[mL/L]**
Glycerin 99.5 %	894.47	
Fill up with deionized water until the final volume is reached		

A.5 Trace Element Solution

The trace element solution was prepared using the recipe showed in Table A.5. After the preparation, the solution was sterilized using filtration, and stored at 4°C.

Table A.5: Recipe for the trace element solution.

Component	**Concentration** [g/L]
FeSO4 x 7 H2O	16.40
MnSO4 x H2O	10.00
ZnSO4 x 7 H2O	1.00
CuSO4 x 5 H2O	0.31
NiCl2 x 6 H2O	0.02
Fill up with deionized water until the final volume is reached	

A.6 Biotin Solution

The biotin solution was prepared using the recipe showed in Table A.6. After the preparation, the solution was sterilized using filtration, and stored at -20°.

Table A.6: Recipe for the biotin solution.

Components	**Concentration** [g/L]
Biotin	0.2
Fill up with 1M NaOH solution until the final volume is reached	

A.7 Protocatechuic Acid or 3,4-Dihydroxybenzoic Acid Solution

The Protocatechuic acid or 3,4-dihydroxybenzoic acid (PCA) solution was prepared using the recipe showed in Table A.6. After the preparation, the solution was sterilized using filtration, and stored at -20°.

Table A.7: Recipe for the PCA solution.

Components	**Concentration** [g/L]
PCA	30
Fill up with 1M NaOH solution until the final volume is reached	

A.8 Minimal Medium

The minimal medium was prepared using the recipe showed in Table A.8. The CGXII salt solution, glucose 40% solution, biotin solution, PCA solution, and trace element solution were prepared according to the recipes previously described. As all components used are sterilized when prepared, no sterilization is needed after the preparation of the minimal medium.

Table A.8: Recipe for the minimal medium solution.

Components	**Concentration [mL/L]**
CGXII	800
Glucose 40%	50
Biotin solution	1
PCA	1
Trace element solution	1
Kanamycin stock	0.5
Tetracycline stock	0.5
IPTG stock	2.5
Sterile water	144

A.9 Complex Medium

The brain hart infusion (BHI) complex medium was prepared using the recipe showed in Table A.9. After the preparation, the BHI solution was sterilized using autoclavation. The sorbitol solution used for the preparation of BHIS, was prepared according to the recipes previously described. The BHI agar was kept at 60°C after preparation.

Table A.9: Recipe for the BHI solution, BHIS solution and BHI agar.

Component	**Concentration [g/L]**		
	BHI	**BHIS**	**BHI agar**
BHI	37	37	37
Sorbitol solution	-	9	-
Agar	-	-	15
Fill up with deionized water until the final volume is reached			

A.10 2TY

The 2TY solution was prepared using the recipe showed in Table A.10. After the preparation, the solution was sterilized using autoclavation.

Table A.10: Recipe for the 2TY solution.

Component	**Concentration [g/L]**
Tryptone	16
Yeast	10
NaCl	5
Fill up with deionized water until the final volume is reached	

A.11 EPB Buffers

The EPB1 and EPB2 buffers were prepared using the recipe showed in Table A.11. Before adding water, the pH was adjusted to 7.2 using 0.1 M NaOH. After the preparation, the buffers were sterilized by autoclavation.

Table A.11: Recipe for the EPB1 and EPB2 buffers.

Components	**Concentrations**		**Units**
	EPB1	**EPB2**	
HEPES	5.05	1.2	g/L
Glycerin 89%	45.75	137	mL/L
Fill up with deionized water until the final volume is reached			

B Calculations

B.1 Dilutions

To calculate the dilutions needed for the preparation of the solutions used in this work, the Equation B.1 was used, where C is concentration and V is volume.

$$C_1 \cdot V_1 = C_2 \cdot V_2 \tag{B.1}$$

B.2 Standard Deviation and Average

For the calculations of the standard deviation S_x, the Equation B.2 was used.

$$S_x = \sqrt{\frac{\sum_{i=1}^{n}(x_i - \overline{x})}{n-1}} \tag{B.2}$$

Here, n is the total number of samples, x_i is the value of sample i, and $\overline{x}$ is the average value of the samples. The average $\overline{x}$ was calculated using Equation B.3.

$$\overline{x} = \frac{\sum_{i=1}^{n} x_i}{n} \tag{B.3}$$

B.3 Biomass Yield

To calculate the biomass yield Y_B, the Equation B.4 was used.

$$Y_B = \frac{\text{Final biomass}}{\text{Mass of carbon source}} \tag{B.4}$$

B.4 OD600 Correlation Factor

To correlate the automatic biomass measurements from the BioLector into actual OD600 values, a OD600 correlation factor (CF_{OD}) was calculated for each fermentation. The OD600 of the finished cultivations, and the average of the final 30 BioLector automatic biomass measurements, were used to calculate CF_{OD} as shown in the Equation B.5. The CF_{OD} was then multiplied by all the automatic biomass measurements, yielding correct OD600 values. The CF_{OD} calculated for each BioLector fermentation is listed in Table C.5.

$$CF_{OD} = \frac{\text{Final OD600}}{\overline{x}_{\text{Measurements}}} \tag{B.5}$$

B.5 Microbioreactor Correlation Factor

To calculate the microbioreactor correlation factor CF_{Micro}, the average growth rates achieved in the BioLector ($\overline{GR}_{\text{Micro}}$) of the control strain CgEmpty grown at optimal conditions, was calculated using Equation B.3. To calculate the average growth rate of CgEmpty during a shake flask fermentation ($\overline{GR}_{\text{Shake flasks}}$) with the same conditions, results from unpublished work were used. All values mentioned are listed in Table C.1. Growth rates in the BioLector fermentation supplemented with 1.0 M NaCl deviate from the other fermentations, and therefore were not used in the calculation of CF_{Micro}. Since the conditions are the same for the control strains across the fermentations, it's reasonable to assume that the deviation comes from technical fluctuation. The CF_{Micro} was calculated using Equation B.6, where it was found to be 1.393.

$$\text{CF}_{\text{Micro}} = \frac{\overline{GR}_{\text{Shake flasks}}}{\overline{GR}_{\text{Micro}}} \tag{B.6}$$

C Raw Data

Table C.1: The growth rate and average growth rate of the shake flask fermentation of CgEmpty from unpublished work, as well as the growth rate, average growth rate, and microbioreactor correlation factor (CF_{Micro}) of the control strain grown without NaCl at 30°C during the BioLector fermentations. The different fermentations are differentiated by their fermentation conditions.

Fermentation Conditions		**Growth rate**			**Average**	**CF_{Micro}**
Temperature	NaCl	1	2	3		
[°C]	[mol/L]		[h^{-1}]		[h^{-1}]	
Shake flask fermentation CgEmpty no salt						
30	0.5	0.3827	0.3735	0.3892	0.3818	-
Microbioreactor fermentations CgEmpty no salt						
30	no salt	0.281	0.297	0.281	0.287	1.332
30	0.5	0.319	0.318	0.306	0.314	1.214
30	1.0	0.147	0.149	0.157	0.151	2.523
30	1.5	0.202	0.298	0.201	0.234	1.633

Table C.2: The OD600 values of the samples taken both during the shake flask fermentation of the strains CgEmpty, CgTmTm, and CgPfTm supplemented with 0.5 M NaCl at 30°C, and during the osmotic shock down process.

Fermentation				Osmotic shock down			
Time	**OD_1**	**OD_2**	**OD_3**	**Time**	**OD_1**	**OD_2**	**OD_3**
CgEmpty with 0.5 M NaCl							
0	0.70	0.80	0.80	**0**	7.50	10.00	6.00
2	0.75	0.65	0.70	**2**	6.50	7.00	4.00
5	0.80	0.80	0.70	**4**	4.50	5.50	3.50
9	1.40	1.30	1.00	**73**	2.90	2.40	1.50
10	1.40	1.60	1.30				
19	7.00	9.00	5.55				
20.5	8.00	11.00	7.00				
CgTmTm with 0.5 M NaCl							
0	0.90	0.90	0.80	**0**	8.00	8.50	6.00
2	0.75	0.70	0.70	**2**	5.50	7.50	5.50
5	0.80	0.60	0.80	**4**	4.50	5.50	3.50
9	1.20	1.10	1.00	**73**	2.30	2.80	2.10
10	1.40	1.40	1.40				
19	7.00	7.00	6.00				
20.5	8.00	8.00	7.00				
CgPfTm with 0.5 M NaCl							
0	0.60	0.70	0.80	**0**	4.00	6.50	6.00
2	0.45	0.60	0.65	**2**	3.00	6.50	5.50
5	0.50	0.80	0.70	**4**	2.00	3.50	3.00
9	0.80	1.30	1.50	**73**	1.30	2.60	2.80
10	0.90	1.40	1.70				
19	4.00	6.50	9.00				
20.5	4.50	8.00	10.50				

Table C.3: The OD600 values measured after the four different fermentations in the BioLector. The strains were cultivated at 30°C and 40°C with no NaCl, and supplemented with 0.5 M NaCl and with 1.0 M NaCl at 30°C. Only the parallels with growth have OD600 values listed.

Strain name	**OD_1**	**OD_2**	**OD_3**	**OD_1**	**OD_2**	**OD_3**
	Cultivated at 30°C			*Cultivated at 40°C*		
CgEmpty	30	28	30	2.0	3.0	2.5
CgTmTm	28	26	28	-	-	-
CgPfPf	28	28	28	-	-	-
CgTmPf	28	30	28	-	-	-
CgPfTm	30	24	30	-	-	-
	Cultivated with 0.5 M NaCl			*Cultivated with 1.0 M NaCl*		
CgEmpty	28	28	30	16	16	15
CgEmpty no salt	22	24	24	-	-	-
CgTmTm	24	24	24	-	-	7.0
CgPfPf	28	28	26	-	-	-
CgTmPf	28	28	18	-	6.0	-
CgPfTm	24	26	28	-	1.0	-

Table C.4: The OD600 measurements of samples taken both during the bench-top bioreactor fermentation of CgTmTm supplemented with 0.5 M NaCl at 30°C, and after the cells were transferred to another bench-top bioreactor with water for an osmotic shock down.

Bioreactor																		
Time [h]	0	2	4	6	12	13	18	20	21	22	24	24.25	25	26	27.25	28.25	29	42.5
OD600	1	1.4	1.6	2	4.4	5.4	11.2	21	20	21	30	34	38	36	32	32	30	28
Osmotic shock down in bioreactor																		
Time [h]	0	1	2	3	4	5	6	7	24.5									
OD600	16	17	13	16	16	16	13	13	13									

Table C.5: The CF_{OD} used to correlate the automatic biomass measurements taken by the BioLector to real OD600 values. The conditions of the different BioLector fermentations are listed.

Strain name	**Correlation factor (CF_{OD})**					
Parallel:	1	2	3	1	2	3
Cultivated with:	*no salt at 30°C*			*no salt at 40°C*		
CgEmpty	0.10178	0.09572	0.10320	0.02259	0.04051	0.03532
CgTmTm	0.09759	0.09247	0.09955	-	-	-
CgPfPf	0.10182	0.10865	0.10586	-	-	-
CgTmPf	0.09996	0.10824	0.10371	-	-	-
CgPfTm	0.10445	0.08589	0.10729	-	-	-
Cultivated with:	*0.5 M NaCl at 30°C*			*1.0 M NaCl 30°C*		
CgEmpty no salt	0.10046	0.10088	0.11084	0.06214	0.06103	0.05926
CgEmpty	0.09706	0.10733	0.10167	-	-	-
CgTmTm	0.09433	0.09054	0.09126	-	-	0.07761
CgPfPf	0.10041	0.09946	0.09202	-	-	-
CgTmPf	0.09882	0.09788	0.06406	-	0.06798	-
CgPfTm	0.09431	0.09852	0.10761	-	0.01313	-

Table C.6: Peak heights from the HPLC analysis of samples taken of the shake flask growth experiment before and after an osmotic shock down, where CgEmpty, CgTmTm and CgPfTm were grown in minimal medium supplemented with 0.5 M NaCl at 30°C.

HPLC peak heights at retention time of 19.9 min					
Strain parallel	Time [h]				
	Before OSD	0	2	4	73
CgEmpty 1	84.6	6.7	7.0	7.1	8
CgEmpty 2	79.6	7.5	7.7	7.7	8.6
CgEmpty 3	86.5	6.5	7.2	7.2	8.3
CgTmTm 1	80.9	8.0	8.1	8.6	9.5
CgTmTm 2	82.3	9.1	9.5	10.7	11.3
CgTmTm 3	82.2	7.7	8.4	8.8	9.8
CgPfTm 1	82.3	7.1	7.2	7.7	8.7
CgPfTm 2	80.9	6.9	7.8	8.0	9.0
CgPfTm 3	81.6	6.5	7.4	7.2	8.4
HPLC peak heights at retention time of 7.1 min					
Strain parallel	Time [h]				
	Before OSD	0	2	4	73
CgEmpty 1	144.3	-	-	-	-
CgEmpty 2	139.8	-	-	-	-
CgEmpty 3	146.9	-	-	-	-
CgTmTm 1	140.8	-	-	-	-
CgTmTm 2	139.8	-	-	-	-
CgTmTm 3	140.0	-	-	-	-
CgPfTm 1	140.1	-	-	-	-
CgPfTm 2	142.0	-	-	-	-
CgPfTm 3	139.4	-	-	-	-

Table C.7: Peak heights at retention times (RT) of 7.1 min, 8.8 min and 19.9 min, from the HPLC analysis of samples taken of the bioreactor growth experiment before and after an osmotic shock down, where CgTmTm was grown in minimal medium supplemented with 0.5 M NaCl at 30°C.

HPLC peak heights from Bioreactor			
Time [h]	RT = 7.1 min	RT = 8.8 min	RT = 19.9 min
Fermentation before osmotic shock down			
0.0	148.9	-	-
2.0	152.8	-	-
4.0	150.4	-	-
6.0	153.9	1.3	-
12.0	151.1	30.5	-
13.0	152.6	31.0	-
18.0	149.6	31.8	-
20.0	152.2	32.8	-
22.0	155.4	33.7	-
24.0	155.3	33.2	-
26.0	149.8	34.4	-
28.3	154.0	37.0	-
29.0	152.1	37.1	-
42.5	153.6	37.6	-
Suspension after the osmotic shock down			
43.5	-	7.2	10.4
44.5	-	8.8	12.9
45.5	-	8.8	13.0
46.5	-	8.9	12.8
47.5	-	9.2	12.8
48.5	-	9.1	12.7
49.5	-	8.4	12.2
50.5	-	9.0	12.1
68.5	-	9.8	12.6

D Nomenclature

Table D.1: Abbreviations and their descriptions used in this work.

Abbreviation	Description
2TY	two triptone one yeast
BHI	Brain hart infusion
BHIS	Brain Hart Infusion with Sorbitol
bps	Base Pairs
CDP	Cytidine Diphosphate
CF_{Micro}	Correlation factor for microbioreactor
CF_{OD}	Correlation factor for fermentation
DIP	Di-*myo*-inositol-phosphate
DIPP	Di-*myo*-inositol-phosphate-phosphate
DIPPS	Di-*myo*-inositol-phosphate-phosphate-synthease
DNA	Deoxyribonucleic Acid
GC	Gas Chromatography
$\overline{GR}_{Micro}$	Avarage growth rate of microbioreactor fermentations
$\overline{GR}_{Shake\ flasks}$	Average growth rate of shake flask fermentations
HiFi PCR	High Fidelity PCR
HPLC	High-performance liquid chromatography
IMP	Di-*myo*-inositol-phosphate-phosphate-phosphatase
IPCT	Inositol-1-phosphate-cytidylyltransferase
IPS	*myo*-Inositol-1-phosphate-synthease
IPTG	Isopropyl β-D-1-thiogalactopyranoside
LB	Lysogeny broth
MS	Mass Spectroscopy
NaCl	Sodium Chloride
NMR	Nuclear Magnetic Resonance
OD600	Optical density at 600nm
OPF	Open Reading Frame
PCR	Polymerase Chain Reaction
pO2	partial pressure of oxygen
POR	Pyruvate ferredoxin oxi-doreductase
RI Detector	Refractive Index Detector
rpm	Revolutions per minute
RT	Retention Time
UVA	Ultra Violet A
UVB	Ultra Violet B
vvm	Volume per Volume per Minute

NTNU

Norwegian University of
Science and Technology